

Surface Characterization of Cricket Balls Using Area-scale Fractal Analysis

by

Omair I Paracha

A Thesis

submitted to the faculty of

Worcester Polytechnic Institute

in partial fulfillment of the requirements for the

Degree of Master of Science

in

Mechanical Engineering

January 2010

Approved:

Professor Christopher Brown
Major Advisor

Professor Simon Evans
Thesis Committee Member

Professor Rajib Mallick
Thesis Committee Member

Professor Cosme Furlong
Graduate Committee Representative

Foreword

Cricket is an old sport. The first recorded cricket match was played at Coxheath in Kent, England in 1646 and the first test match took place in Melbourne, Australia in 1877 between England and Australia. The Ashes series (played between Australia and England) is being organized since 1877 (Mehta, 2005). During the last century the sport has spread to over 100 countries. The governing bodies of various member countries earn millions of dollars every year from marketing and organizing cricket tournaments. Cricket Australia's annual revenue for the year ending in June 2008 was close to a \$ 134 million.

The playing performance of cricket balls is one of the most important parts of a match. A faulty ball can favor one team and hence result in a loss of big sums of money for the opponents, not to mention the grief over that loss. Hence cricket ball manufacturers have to make sure that the behavior of every ball being used during the course of a tournament is similar, if not exactly the same. Wear and tear of a cricket ball is expected but they should last for a certain period of time (50 overs for a one day match and 90 overs for a test match). If a ball loses its shape, color or shine or the seam lifts up earlier than normal; it is required to be replaced which under certain conditions might not be one of the team's preference based on if they are batting or bowling. For instance a white cricket ball is hard to see if mud or starts to stick to it and batsman like to have it changed but bowlers are not happy with that because a fresh ball (although used for the same number of overs) might be a bit hard which travels faster through the outfield and it becomes easy to score runs.

It is a well know fact that surface roughness affects the playing performance of a cricket ball A new ball is made to swing by the bowlers by varying the position of the seam but as it grows older the seam becomes softer and lifts up which reduces the amount of swing produced. This type of swing is generated after the ball bounces off the ground and is called conventional swing. The bowling side tries to shine the ball to delay this process of wear and tear. The ball can be made to swing once it gets old by keeping one side smooth and letting the other become rough. This type of swing takes place before the ball bounces off the ground and is the primary reason for the toe crushers or in swinging yorkers bowled by fast bowlers. It is called reverse swing. From experience bowlers know that a ball starts to reverse swing around the thirty fifth over for a medium pace bowler. Bowlers who can generate speeds higher than 90 mi/hr can make the ball to reverse swing as early as the 15th over.

It's not uncommon for people in academia to show interest in physical phenomenon related to the sport of cricket. Conventional swing and reverse swing both remain an interesting subject of study for scientists. The relationship between surface roughness and the aerodynamic behavior has been investigated in the past. The present work is an attempt to quantify the surface roughness of cricket balls which has not been previously done.

Abstract

Cricket balls behave differently at various stages of the game depending upon how much wear and tear has taken place due to use. The playing performance of cricket balls depends largely on the surface texture. The ball is swung using the primary seam during the early stages of the game but later the surface roughness starts to affect the lateral movement. This work attempts to find a quantitative measure of the surface roughness of cricket balls and then uses it to discriminate between new and old balls. Area-scale fractal analysis is used to find the surface roughness in order to discriminate between the balls. FTEST (a statistical tool) is also used to establish a discriminatory criterion between the old and new balls. Wind tunnel test results are presented to show the relationship between the surface roughness and drag. Finally a correlation between the roughness and drag of the cricket is shown.

Acknowledgements

I would like to thank my advisor Professor Christopher Brown for encouraging me to take up a project related to my personal interests. His consistent support made it possible for me to produce this work.

To Professor Simon Evans for his valuable comments on the work and suggestions to improve the second part of the report related to aerodynamics

To Professors Ryszard Pryputniewicz, Mark Richman, Mikhail Dimentberg, Mahadevan Padmanabhana and Cosme Furlong for mentoring me while I worked under them me as a teaching assistant.

Special thanks to Brendan Powers for the valuable discussions on surface metrology. Without him this project would have been tough to handle.

Table of Contents

Foreword	2
Abstract	4
Acknowledgements	5
List of figures	9
Nomenclature	12
1. Introduction	14
1.1 Objective	14
1.2 Rationale	14
1.3 State of the art	15
1.4 Approach	17
2. Methods	19
2.1 Measurements	19
2.1.1 Surface metrology measurement	19
2.1.2 Wind tunnel tests	20

2.2	Filtering	21
2.3	Analysis	22
2.3.1	Area-scale fractal analysis	22
2.3.2	FTEST	25
3.	Results	27
3.1	Measurements	27
3.1.1	New ball	27
3.1.2	50 over old ball	28
3.1.3	30 over old ball	39
3.2	Conventional parameters	30
3.3	Height maps	32
3.4	Area-scale fractal analysis	36
3.4.1	New ball	36
3.4.2	30 over old ball	39
3.4.3	50 over old ball	43

3.5	Comparison of Area-scale fractal analysis	46
3.6	FTEST	49
3.7	Wind tunnel tests	52
3.8	Relationship between drag and roughness	53
4.	Discussion	57
5.	Conclusion and future recommendations	60
	References	62

List of figures

Figure-2.1: The wind tunnel for drag studies	20
Figure 2.2: The 50 over old ball in the wind tunnel for drag measurements	21
Figure 2.3: Virtual tiling of a measured surface	23
Figure 2.4: Area-scale plot for a new cricket ball at 135 Degrees location around the circumference	24
Figure 3.1: Micrographs of the new ball	27
Figure 3.2: Micrographs of the 50 over old ball	28
Figure 3.3: Micrographs of the 30 over old ball	29
Figure 3.4: Means of arithmetic average height	31
Figure 3.5: TTEST results for the cricket balls based on S_a	32
Figure 3.6: New ball-315 degree, 3D height maps of the ball showing the decrease in spikes after filtering	33
Figure 3.7: 30 over old ball-220 degree, 3D height maps of the ball showing the decrease in spikes after filtering	34
Figure 3.8: 50 over old ball-center, 3D height maps of the ball showing the decrease in spikes after filtering	35

Figure 3.9: New ball, Area-scale-unfiltered	36
Figure 3.10: New ball, Area-scale with spike removal	37
Figure 3.11: New ball, Area-scale with Gauss filter	38
Figure 3.12: 30 over old ball, Area-scale, unfiltered	40
Figure 3.13: 30 over old ball, Area-scale with spike removal	41
Figure 3.14: 30 over old ball, Area-scale with Gauss filter	42
Figure 3.15: 50 over old ball, Area-scale-unfiltered	43
Figure 3.16: 50 over old ball, Area-scale with spike removal	44
Figure 3.17: 50 over old ball, Area-scale with Gauss filter	45
Figure 3.18: Comparison of Area-scale, mean, unfiltered	46
Figure 3.19: Comparison of Area-scale mean with spike removal	47
Figure 3.20: Comparison of Area-scale with Gauss filter	48
Figure 3.21: FTEST, mean, Area-scale, new vs. 30 with 90% confidence	49
Figure 3.22: FTEST, mean, Area-scale, new vs. 50 with 90% confidence	50
Figure 3.23: FTEST, mean, Area-scale, 30 vs. 50 with 90% confidence	51
Figure 3.24: Velocity vs. drag for the cricket balls	52

Figure 3.25: Regression plot showing the calculation of R2 for drag vs. relative area	54
Figure 3.26: Drag at different velocities vs. relative area	55
Figure 3.27: C_D at different velocities vs. relative area	56

Nomenclature

A	Area of the cricket ball
C_D	Coefficient of drag
F_D	Drag
FTEST	A continuous probability distribution which describes the probability of the value falling within a particular interval
ρ	Density of air
P_{ai}	Projected area for the virtual tile
R_{ea}	Relative area
R^2	Coefficient of correlation
Sampling Interval	The distance between two measurements taken by the laser scanning microscope
Sampling Region	The total area measured by the laser scanning microscope
S_a	The arithmetic average height parameter for an area
V	Velocity of air

θ

The angle that the normal to the measurement tile makes with the normal to the datum plane for the tiling exercise.

Chapter 1

Introduction

1.1 Objective

The objective of this work is to characterize the surface roughness of cricket balls, to find a quantitative measure of the roughness and use that information to discriminate between new and 30 over old balls and finally to find a functional correlation between the roughness and aerodynamic behavior of new and old cricket balls.

1.2 Rationale

The surface roughness of cricket balls is the most important factor which determines the amount of swing produced once the ball starts to wear and tear. Pitch conditions, weather and the nature of the outfield all change the surface texture of a ball over the course of the game. Although scientists have discussed the aerodynamic performance of cricket balls as a result of this wear and tear but a quantitative measure of the surface roughness of cricket balls was not found in the literature. This work is an attempt to fill that void. Using the information about surface roughness of new and 30 over old balls, an attempt is made to discriminate between them. Finding a functional correlation between the surface roughness and the aerodynamic performance which is the second objective of this study is accomplished by presenting wind tunnel drag measurements for the new and 30 over old balls.

1.3 State-of-the-art

Scientists as early as the seventeenth century studied the curved flight of a tennis ball (Newton, 1672; Rayleigh, 1877). Spin bowlers in cricket also use this type of spin to generate the “Magnus effect” (Mehta and Wood, 1980). The subject of the present study however, is another type of swing (hence the terms “swing bowling”) and the effect of a change in surface texture of the cricket ball due to wear and tear during the course of a match. This type of swing is unique to cricket due to the presence of a seam and the fact that the ball bounces on the ground before coming in contact with the bat.

Cook (1955) was the first to publish a paper on cricket ball swing explaining the reason for a new shiny ball to swing more as compared to an old one using the boundary layer flow theory. Lyttleton (1957) and Mehta et al. (1980) have also come up with theories about cricket ball swing. Barton (1982) and Mehta et al. (1983) described their experimental findings explaining the factors affecting the magnitude of side force that generates swing.

An extensive study on the surface roughness of cricket balls was not found in the literature although Mehta et al. (1983) investigated the effects of humidity by presenting Talysurf contour plots of the primary seam. In the same paper they explained the effects of surface roughness on the aerodynamic performance of cricket balls. They measured the force on spinning cricket balls by rolling them along their seam down a ramp and projected in a wind tunnel. The aerodynamic forces were calculated from the measured deflections. They measured an increase in the side force when the when the seam was set

at an incidence to the oncoming flow. The critical velocity at which the side force started to decrease was about 30 m/s ($Re = 140,000$). They argued that this was the velocity at which the laminar boundary layer on the non seam side undergoes transition and becomes turbulent.

Mehta et al. (1993) showed results from wind tunnel tests in order to explain reverse swing. They showed that at a high bowling speed (over about 85mph for a new ball) the laminar boundary layer transitions into a turbulent state before reaching the seam location. This makes the boundary layer thicker and weaker and it therefore separates earlier than the turbulent layer over the bottom surface. This means that the side force is going to be on the opposite side of what is expected. The fastest bowlers in the world who bowl at over 90 mph will thus only produce reverse swing. As the roughness on this leading side is increased, the critical bowling speed above which reverse swing can be obtained is reduced. This is the primary reason for reverse swing to come into play with older balls.

Haake et al. (2007) showed that the performance of sports balls (soccer, tennis and golf) is characterized by the position of the separation points on the surface of the ball, and at a given Reynolds number and spin rate these separation points are influenced by the surface roughness. They found out that the ratio of surface asperity dimension to the diameter was unable to predict the transition from laminar to turbulent flow for different sports balls. They also considered the effect of surface roughness on spin rate decay and found out that tennis balls had spin decay six times that of golf balls due to the increased skin friction.

James et al. (2004) investigated the playing performance of cricket pitches. Three factors namely pace, bounce and consistency are important in this respect. The surface texture of a cricket ball is altered by a pitch due to the soil type and the amount of grass in it. Correlations were drawn between the pitch performance and the soil composition.

1.4 Approach

From the literature survey it was concluded that laser scanning microscopy has never been used to obtain height maps of the surface of cricket balls. Using a fractal analysis approach these height maps can be used to find the surface roughness. This is the approach adopted in this work.

Chapter 2 of this report discusses the measurement and analysis methods used in the present study. Surfaces of three cricket balls were measured using an OLYMPUS LEXT-3100 laser scanning microscope. The height maps are then thresholded using MOUNTAINS. There are two filtering techniques used which are discussed in this chapter. Area-scale fractal analysis and FTEST are used to discriminate between the balls. A brief introduction about both methods is given. Wind tunnel tests setup is also discussed in this chapter which was used to make drag measurements.

Chapter 3 discusses the results of the measurements and analysis. Difference in height maps for the new and old new balls is discussed. Conventional surface roughness parameters for the three balls are also presented to establish a discriminatory criterion. Area-scale analysis plots and FTEST plots are presented and the difference in surface

roughness of the new and 30 over old balls is discussed. Wind tunnel results showing the relationship between drag and surface roughness are also presented.

Chapter 4 sums up all the results and correlates the findings with the playing performance of cricket balls. Aerodynamic studies from the literature are also discussed to compare the present study and the previous work done in this regard. The onset of turbulent boundary layer is discussed in relation to the 30 over old ball which tends to produce the highest reverse swing.

The final chapter presents the conclusions based on the methods and results presented in previous chapters.

Chapter 2

Methods

2.1 Measurements

2.1.1 Surface metrology measurements

Measurements were made for regions 1275 μm x 975 μm at 1.25 μm sampling intervals using an OLYMPUS LEXT 3100 laser scanning microscope. The measurement region and sampling interval are chosen by the OLYMPUS itself. LEXT 3100 has six objective lenses that can be used to make measurements. OLYMPUS suggests the use of 50X or 100X lenses for good quality measurements but topographic maps obtained by using those resolutions had a large number of lost points hence all measurements were taken at 10X resolution.

The spherical shape of the balls made it difficult to make quality measurements for large regions. Even for small regions the surface curvature came into play. The challenge was to find the top of the ball for any orientation before starting the measurement. For highly rough spots on the 30 over old balls it was sometimes impossible to take a quality measurement even at the top of the ball (for a certain orientation).

2.1.2 Wind tunnel tests

Three cricket balls were used for this study. The balls were drilled and a metal bar was inserted in the hole in order to mount them in the wind tunnel. Figure 2.1 shows the wind tunnel which was used for the measurements.



Figure 2.1: The wind tunnel for drag studies

All the balls were tested with seam perpendicular to the flow as shown in figure 2.2. Tests were run for a range of velocities from 102 ft/s – 139 ft/s which are equivalent to 70 mi/hr and 95 mi/hr respectively.

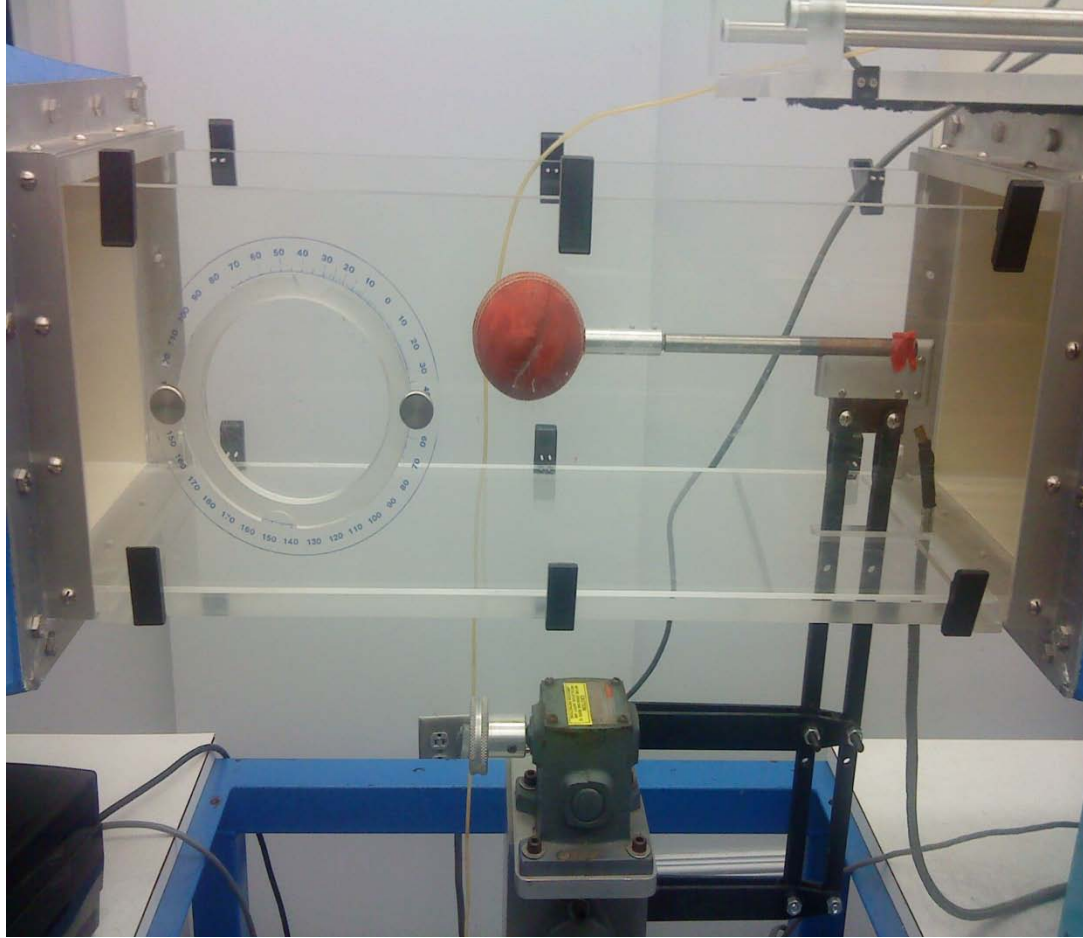


Figure 2.2: The 50 over old ball in the wind tunnel for drag measurements

The data acquisition system of the wind tunnel provided values for drag, pitching moment and lift. Drag was the primary parameter used in this study to calculate coefficient of drag.

2.2 Filtering

Spike removal tool in OLYMPUS was used to remove the valleys generated due to unmeasured points in cracks. Mountains was then used to level and threshold the height maps. A 5 μ m Gauss filter was applied in order to remove the peak and valleys.

The Gauss filter used in MOUNTAINS is an international standard and its details can be found in ISO 11562-1996. It's a phase correct profile filter which is used to separate the long and short wave content of a surface profile.

2.3 Analysis

SFRAX is a software developed in the WPI Surface Metrology Lab under the supervision of Dr. Christopher Brown. It provides the user with a GUI to carry out scale based fractal analysis, FTEST, complexity analysis, variable correlation and digs and scratches analysis. Area-scale Fractal Analysis using FTESTS were performed on the height maps obtained from LEXT 3100.

2.3.1 Area-scale fractal analysis

Conventional surface metrology parameters such as S_a , S_{ku} , S_q do not provide enough information to establish functional correlations. Area-scale fractal relations can help refine the data and testing models. Fractal geometry shows that the area of a surface depends upon the scale of observation. It increases with a decrease in scale. Fractal analysis can be useful in establishing a functional correlation if it is known that the understudy interaction with surface depends upon area.

In Area-scale analysis by the patchwork method (Brown et al. 1993) the scale of measurement is the area a triangular patch used to tile the surface to determine its apparent area at the Area-scale. Figure 2.3 shows the virtual tiling method for four different scales.

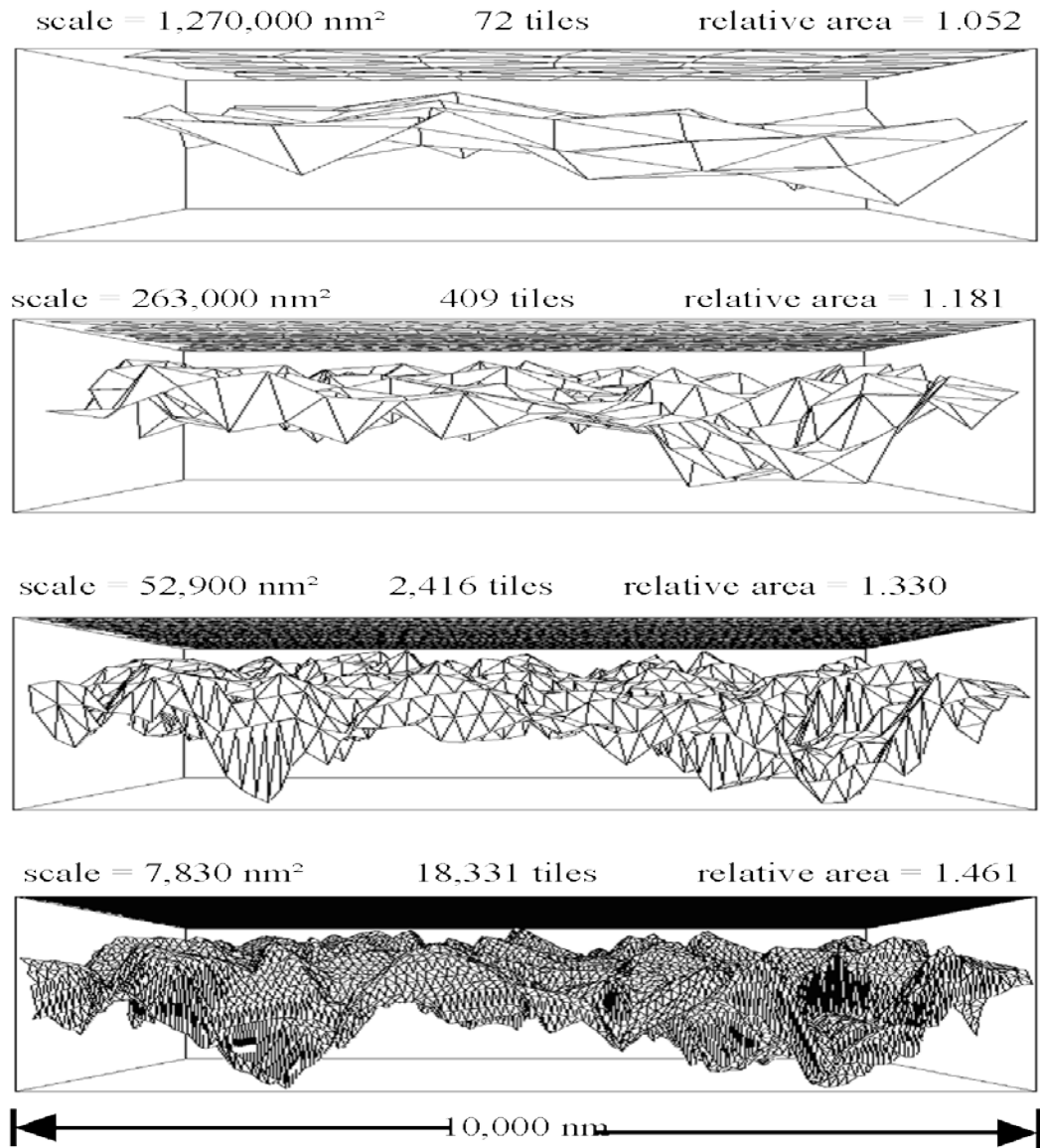


Figure 2.3: Virtual tiling of a measured surface, (From Brown (2005). Produced with permission from the author)

Relative area is used as indication of the physical slopes of the actual surface. The slope of the surface increases as the scale of measurement decreases. The relative areas are equal to a weighted average of the reciprocal of the cosine of the angle that the normal to the measurement tile makes with the normal to the datum plane.

$$R_{ea} = \sum_{i=1}^N \left(\frac{p_{ai}}{A} \right) \left(\frac{1}{\cos \theta_i} \right)$$

Where p_{ai} is the projected area for the virtual tile, i corresponds to θ_i (Brown, et al., 1996). The profile characterization parameters are obtained from a log-log plot of the relative area versus the scale of observation. Figure 2.4 shows a plot like that.

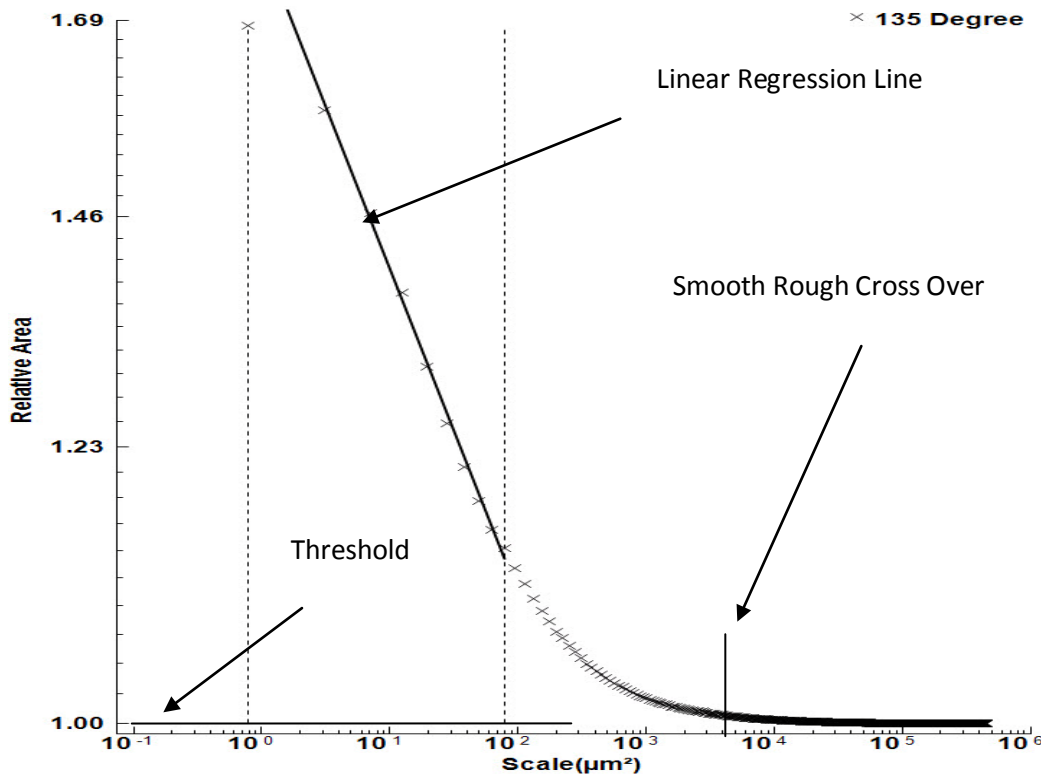


Figure 2.4: Area-scale plot for a new cricket Ball at 135 degrees location around the circumference

The relative areas are approximately 1 at larger scales. As the scale decreases the relative area becomes significantly greater than 1. The scale at which this change takes place is called the smooth rough cross over (SRC). The value of relative area which is considered significantly greater than 1 is called the threshold.

2.3.1 FTEST

The FTEST is a method of analysis of variance. When several sources of variation are acting simultaneously on a set of observations, the total variance is the sum of the variances of the independent sources. Thus the total variation within an experiment is broken down into variations due to each main factor, interacting factors and the experimental error. (Lipson and Sheth (1973)).

The variance for all P samples, with n observations is first calculated as

$$s_i^2 = \frac{\sum_{j=1}^n (x_{ij} - \bar{x}_i)}{n - 1}$$

Where;

s^2 = Mean variance or mean square

n = number of observations

x = the individual observations ranging from $i = 1, 2, \dots, n$

Then the average of all variances is estimated by using the equation

$$\sigma^2 = \frac{\sum_{i=1}^P (s_i^2)}{P}$$

The mean square in this study is plotted against the scale in order to establish a confidence level to discriminate between the two populations. For a certain confidence there is a corresponding minimum mean square value. In the FTEST plots if we observe

the mean square value to be above that value, the two populations can be discriminated with that particular confidence level.

Chapter 3

Results

3.1 Measurements

Micrographs for the new, old and 50 over old ball are presented here.

Measurements for each ball are taken around the circumference at different locations excluding the seam.

3.1.1 New ball

Micrographs for the new ball are presented in figure 3.1.

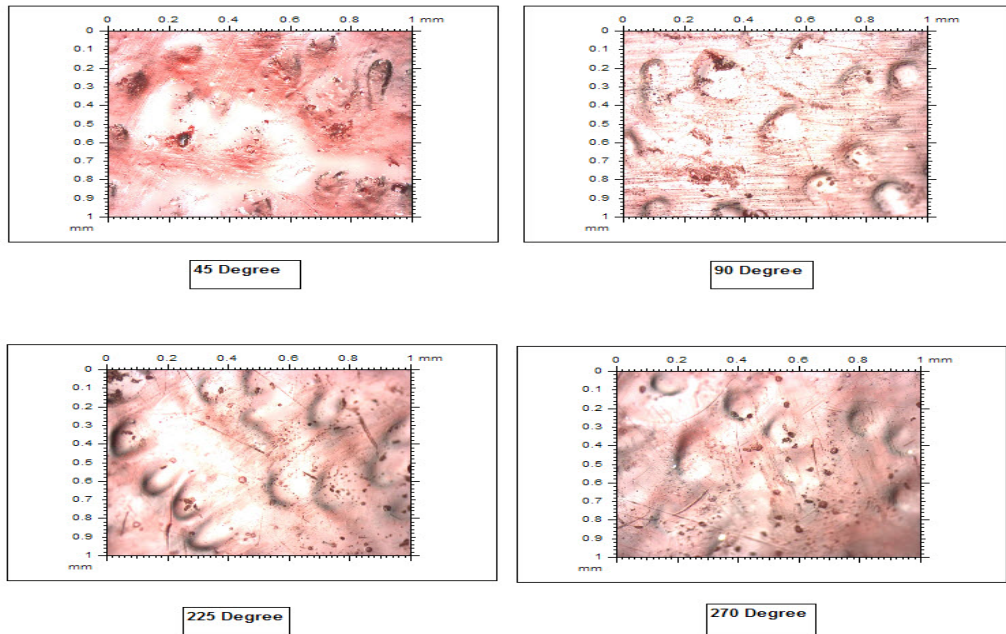


Figure 3.1: Micrographs of the new ball

Four different locations are picked for the measurements which are marked in the figure. The surface texture at these different locations around the circumference of the ball looks quite similar.

3.1.2 50 over old ball

The 50 over old ball has three regions similar in texture. The center location has a shiny silver color which shows that traces of the golden writing present on the ball when it's new. The rest of the surface is rougher and similar in texture.

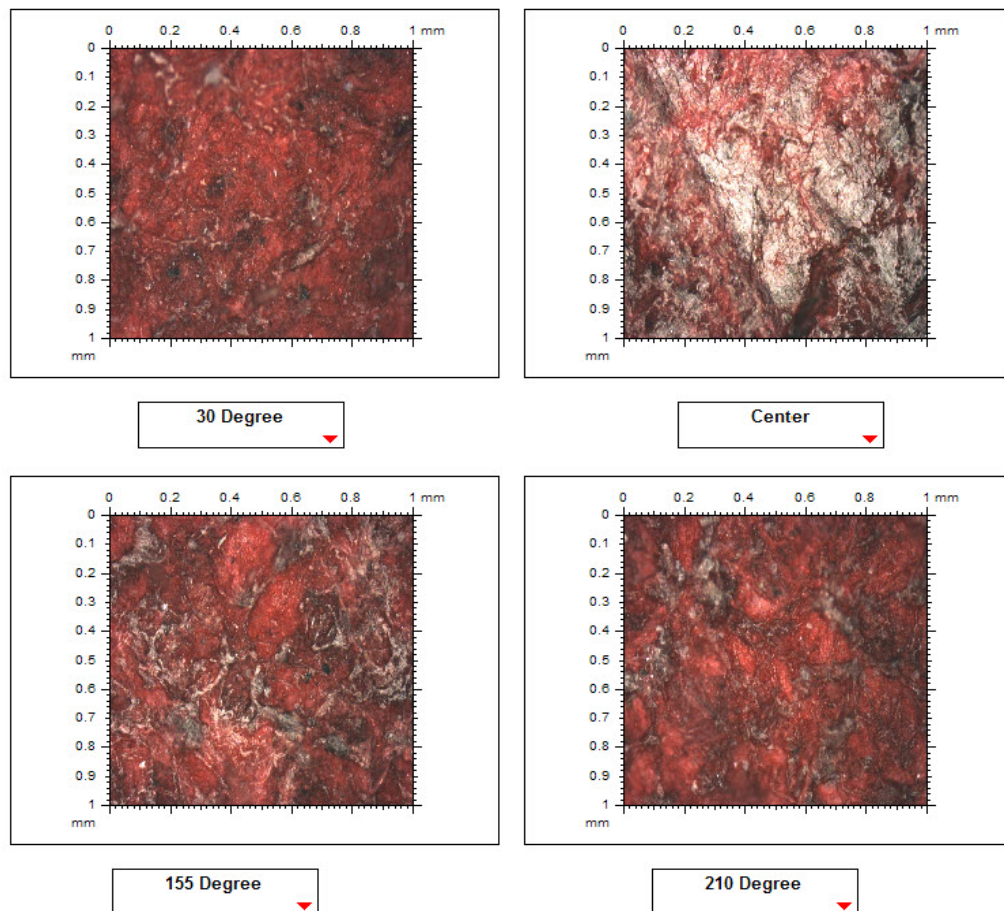


Figure 3.2: Micrographs of the 50 over old ball

3.1.3 30 over old ball

Figure 3.3 shows the micrographs for the 30 over old ball. It has some smooth and some rough regions which show the transition from a shiny surface to the used one. Some regions have a texture similar to the new ball and some to the 50 over old ball. The 90 degree region shows the propagation of cracks. The 270 degree region shows the next step in the change in surface texture with half of a region similar to the new ball

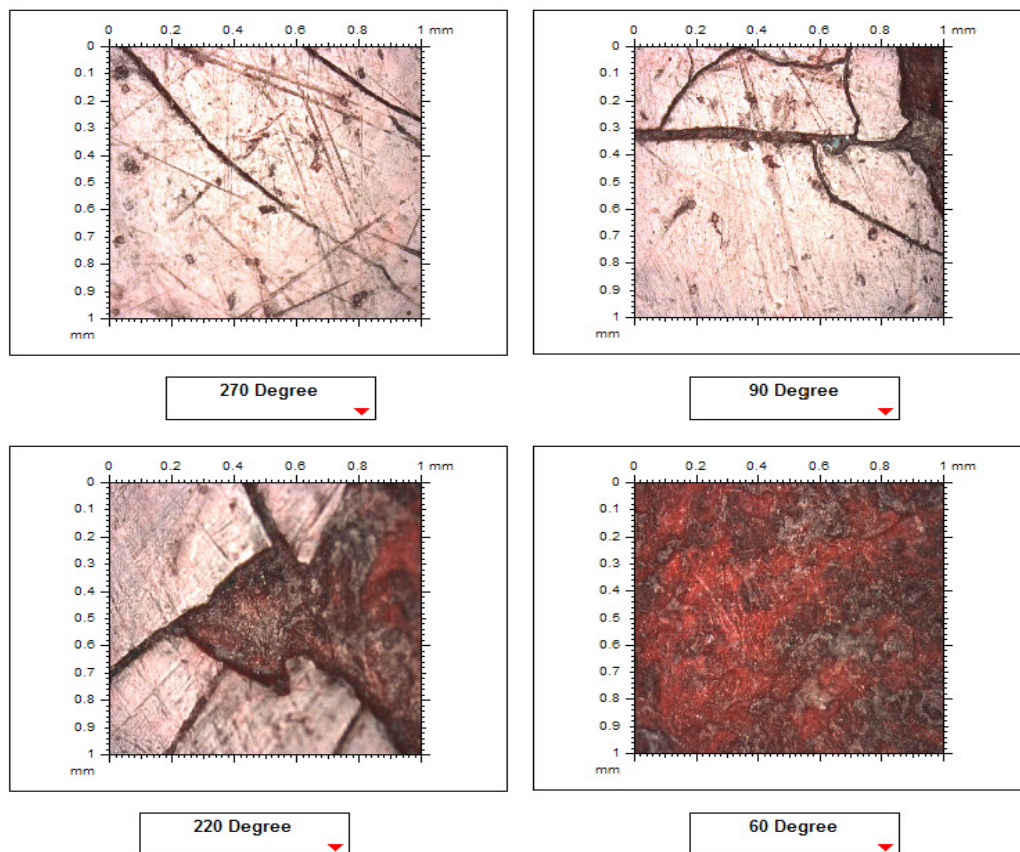


Figure 3.3: Micrographs of the 30 over old ball

and a dark colored region. The 60 degree region shows the absence of the shiny surface and the texture looks similar to the 50 over old ball. It's evident that the shiny surface

tends to crack and then comes off the ball in chips which results in a dull appearance for the 50 over old ball once this process has completed.

3.2 Conventional parameters

In this section the means of S_a which is the arithmetic average height for a surface are presented for the three different balls. S_a is defined as

$$S_a = \frac{1}{mn} \sum_{k=0}^{m-1} \sum_{i=0}^{n-1} |z(x_k, y_l)|$$

Where:

x and y are the two axis of the region being studied.

z is calculated as a function of x and y .

S_a computes the arithmetic average height of the peaks and valleys in the surface.

Figure 3.4 shows the means of S_a for the three different balls for the unfiltered, after spike removal and after Gauss filter measurements. It's evident that S_a decreases after the application of filtering techniques.

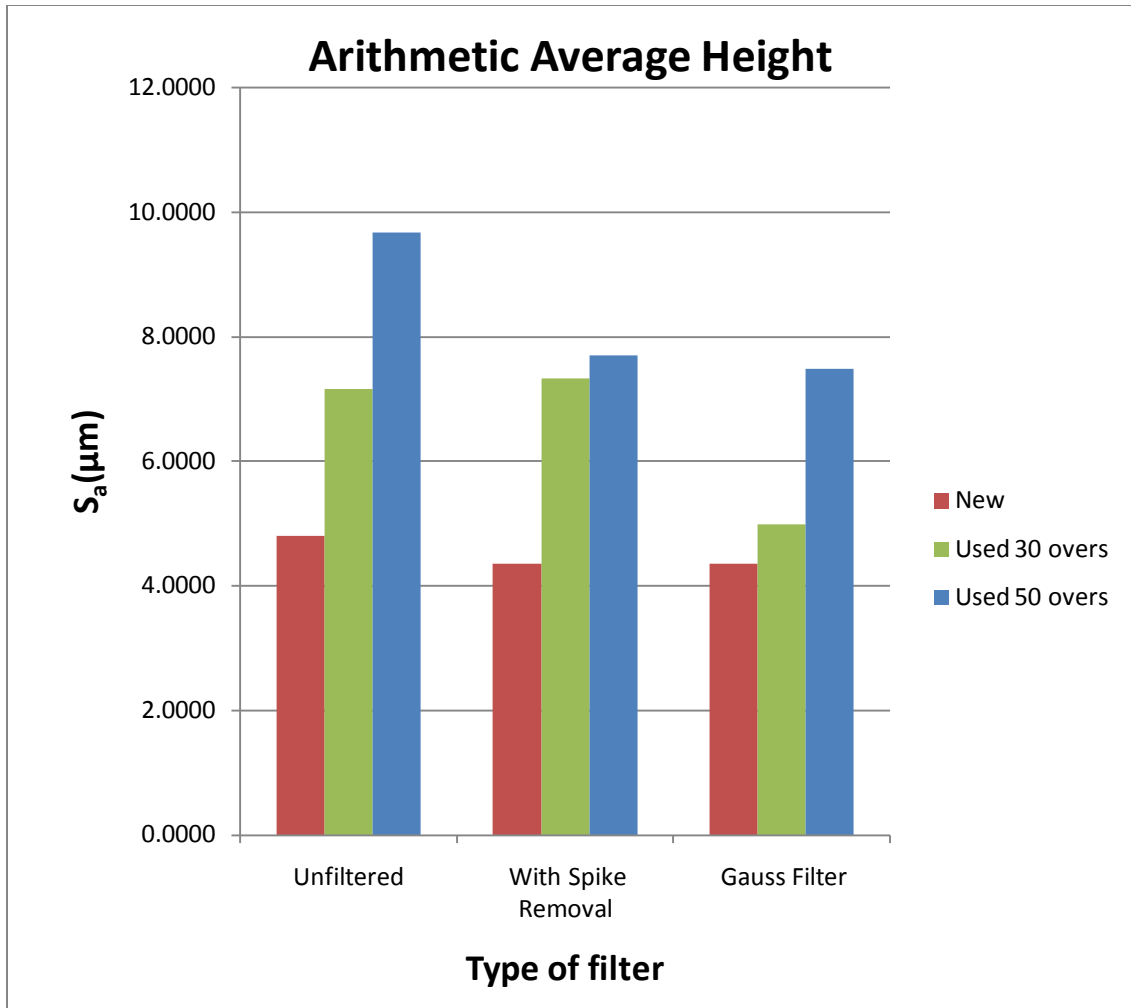


Figure 3.4: Means of arithmetic average height

In order to establish a discriminatory criterion between the balls, a statistical method known as the TTEST was performed on these results using Microsoft Excel. Details about the method can be found in Lipson and Sheth (1973).

Figure 3.5 shows the TTEST results for the three balls. It's a matrix that shows the probability of any two particular balls being similar. The green color shows low probabilities or in other words instances where the two balls can be discriminated with 90%

confidence. The two values in red color show high probabilities of the the balls being similar

	Unfiltered	Spike Removal	Gauss
New vs 30	0.07459	0.07681	0.27701
New vs 50	0.00013	0.00119	0.00159
30 vs 50	0.07480	0.42641	0.03301

Figure 3.5: TTEST results for the arithmetic average height

3.3 Height maps

3D height maps for the new, old and 50 over old ball are given in the following figures in order to show the affect of filtering techniques on the quality of images after spike removal. Figure 3.6 shows the results for a new ball. The unfiltered height map has spikes which can be seen reduced after two filtering steps. The Gauss filter removes the most spikes.

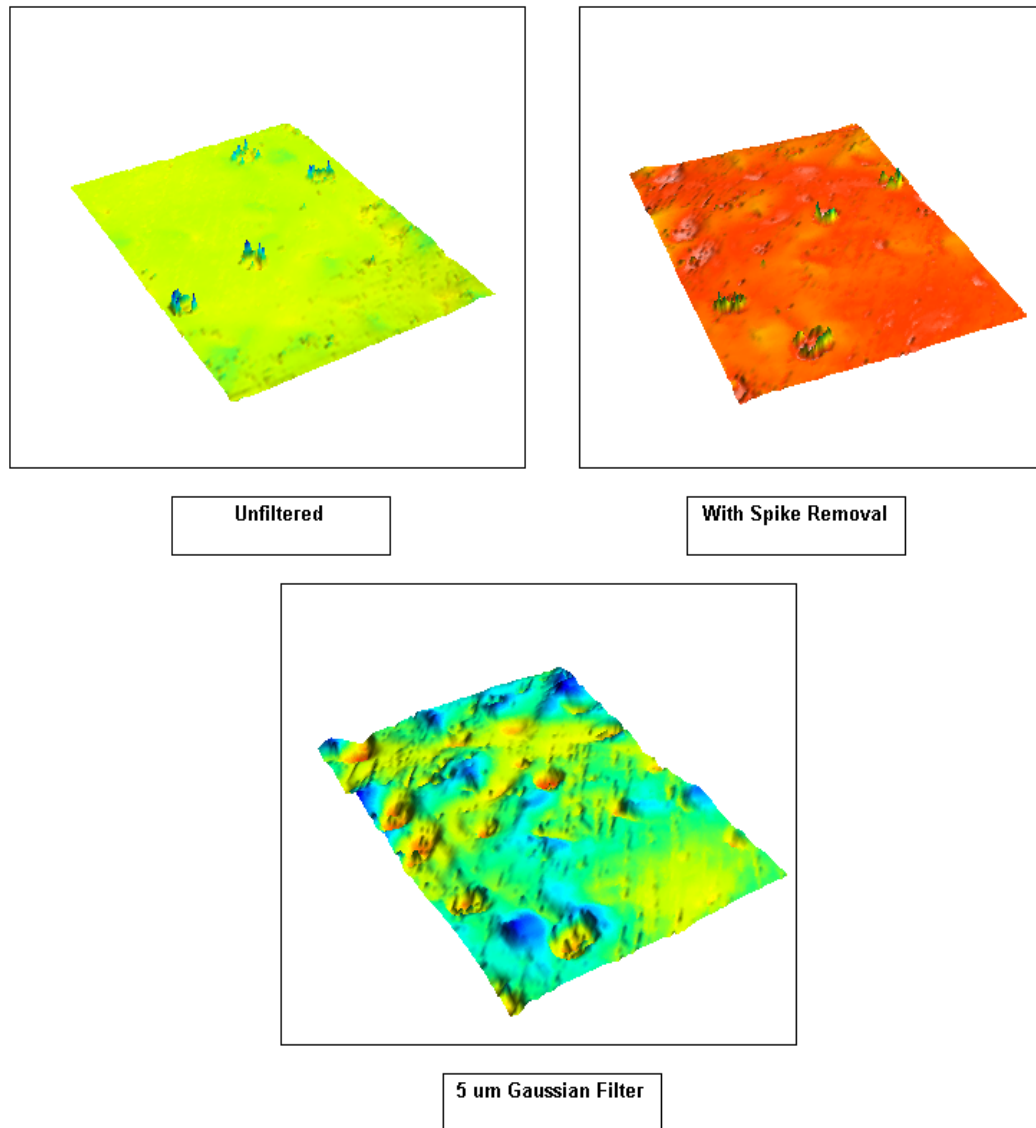


Figure 3.6: New ball-315 degree, 3D height maps of the ball showing the decrease in spikes after filtering

Figure 3.7 shows the height maps for a 30 over old ball. Once again the number of spikes is significant when unfiltered and are significantly reduced after filtering.

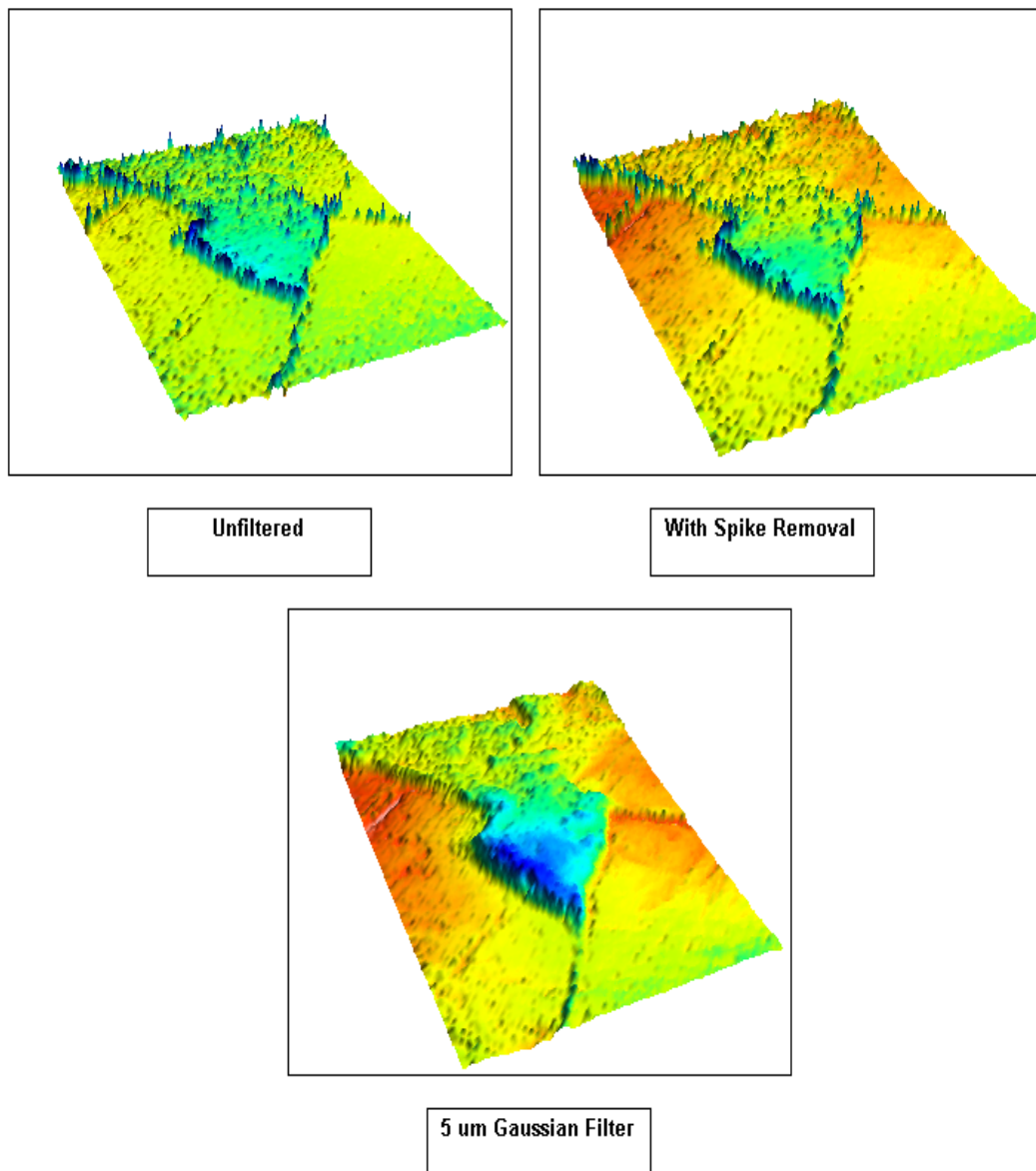


Figure 3.7: 30 over old ball-220 degree, 3D height maps of the ball showing the decrease in spikes after filtering

Figure 3.8 shows the 3D height maps for the 50 over old ball. This measurement has the highest number of spikes as compared to the new and 30 over old ball but the spikes are significantly reduced after filtering.

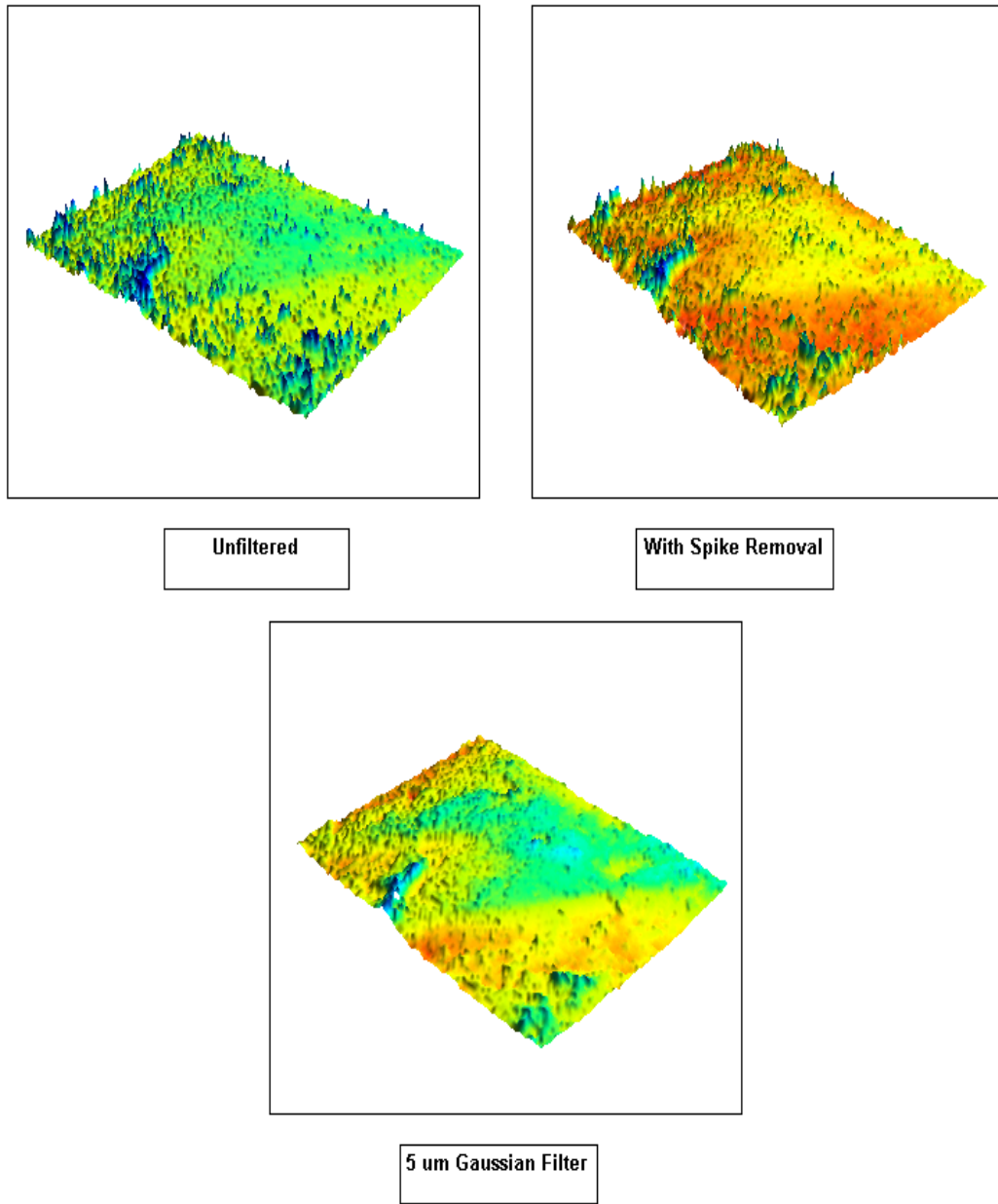


Figure 3.8: 50 over old ball-Center, 3D height maps of the ball showing the decrease in spikes after filtering

3.4 Area-scale fractal analysis

Area-scale fractal analysis is performed for the new, old and oldest and the unfiltered and filtered results are compared.

3.4.1 New ball

Figure 3.9 shows the Area-scale plot for the new ball without any filtering employed. The surface looks rough according to the fractal analysis. A relative area

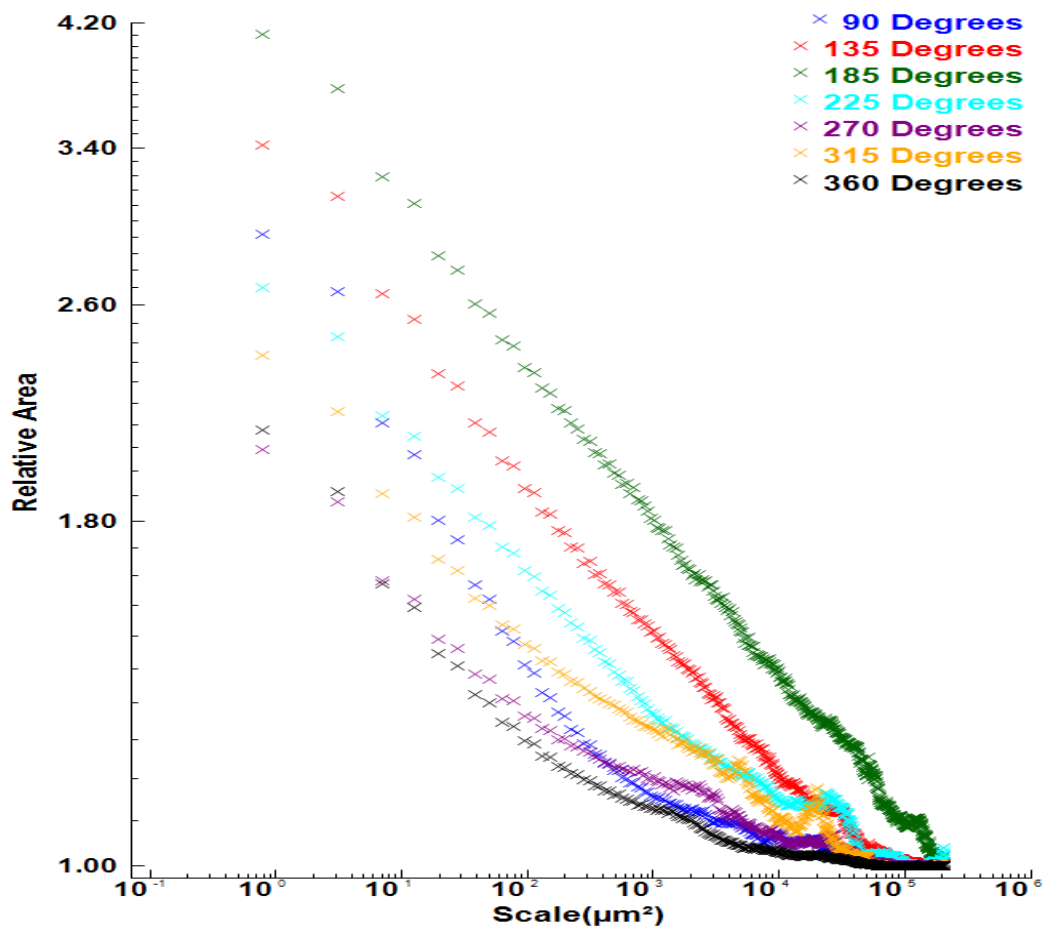


Figure 3.9: New ball, Area-scale, unfiltered

higher than 2 shows that there are too many unmeasured points. At higher scales the values of relative areas decrease after an increase. This is evident for the 315 degree measurement. It shows that the surface has some unmeasured points. At finer scales different regions have different relative areas but the values of relative areas are high as mentioned before and the difference in relative areas for the different regions is also high.

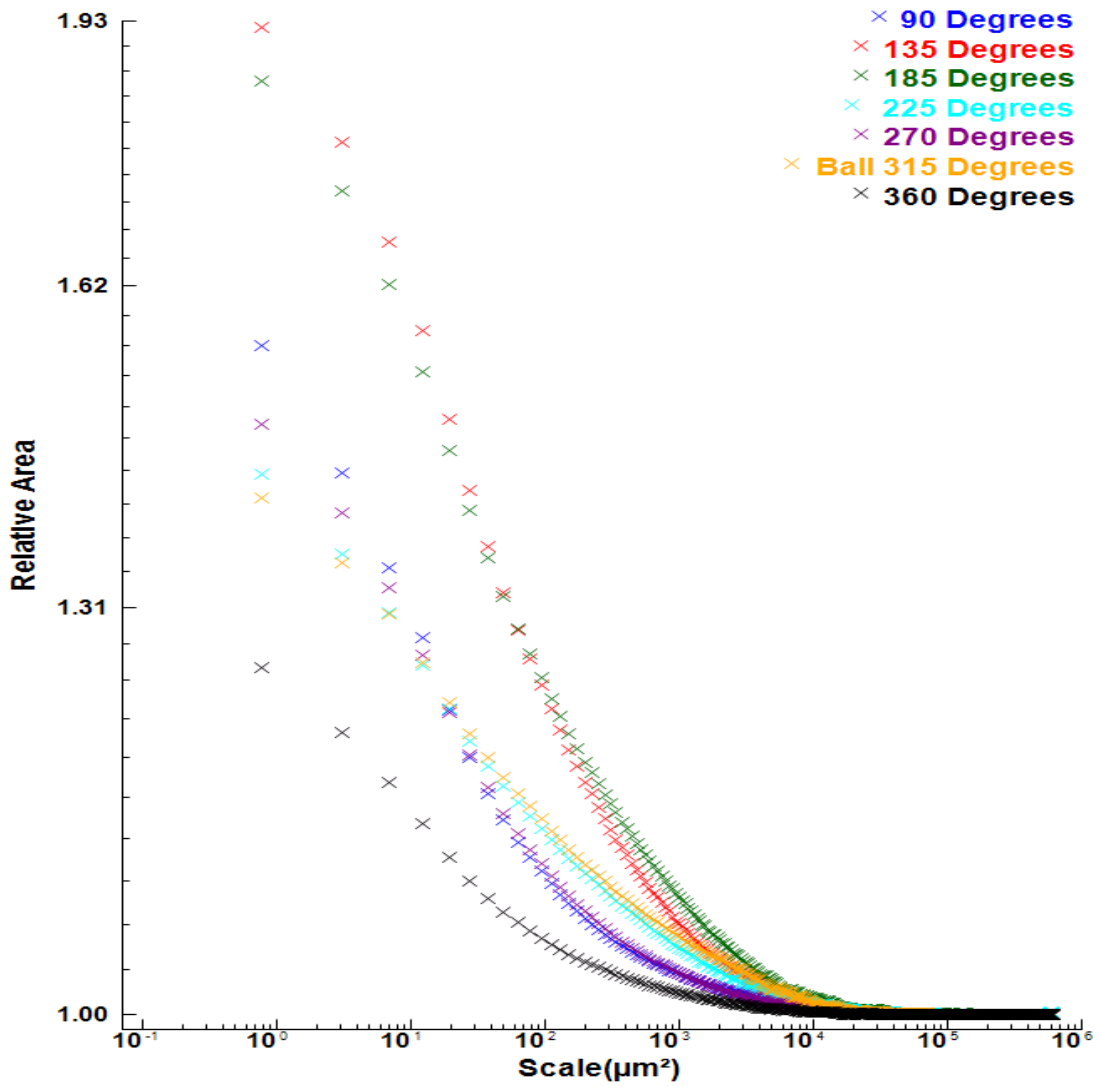


Figure 3.10: New ball, Area-scale with spike removal

Figure 3.10 shows the results of Area-scale fractal analysis for the same ball but after employing the spike removal tool from OLYMPUS. The curves are much smoother and the values of relative areas for all results are below 2 which show that the spike removal tool did successfully remove some spikes. The difference in values of relative areas has also decreased.

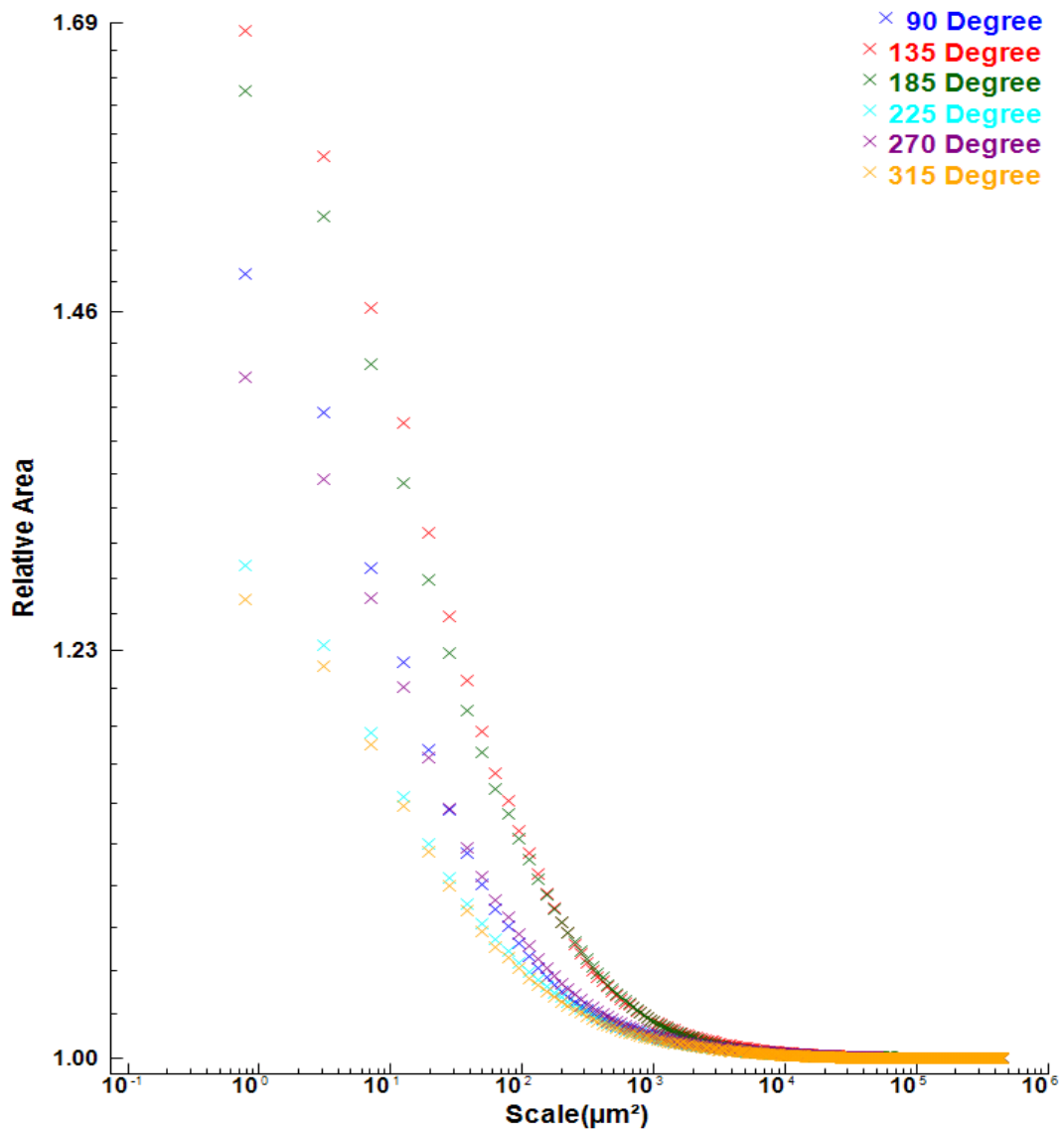


Figure 3.11: New ball, Area-scale with Gauss filter

Figure 3.11 shows the Area-scale plot for the same ball after employing a 5um Gauss filter using MOUNTAINS. The relative area values have decreased further and the difference in values of the relative area has also decreased. It shows that the ball has a lowest relative area value of 1.25 for the 315 degree measurement and the highest value of 1.69 for 135 degree measurement. The Gauss filter removes most of the spikes and makes it possible to characterize the actual texture of the surface.

3.4.2 30 over old ball

Area-scale fractal analysis results for the 30 over old ball are shown in the following three plots. Figure 3.12 shows the unfiltered results.

As mentioned earlier and shown with the help of micrographs and height maps, the 30 over old ball has some regions similar to the new and some regions similar to the 50 over old ball. The smoothest region on the 30 over old ball has the highest relative area of 3.8.

This value is close to the highest relative area of 135 degree measurement for the new ball (unfiltered). All Area-scale results in the plot have an unrealistic relative area which shows the presence of too many spikes or unmeasured points.

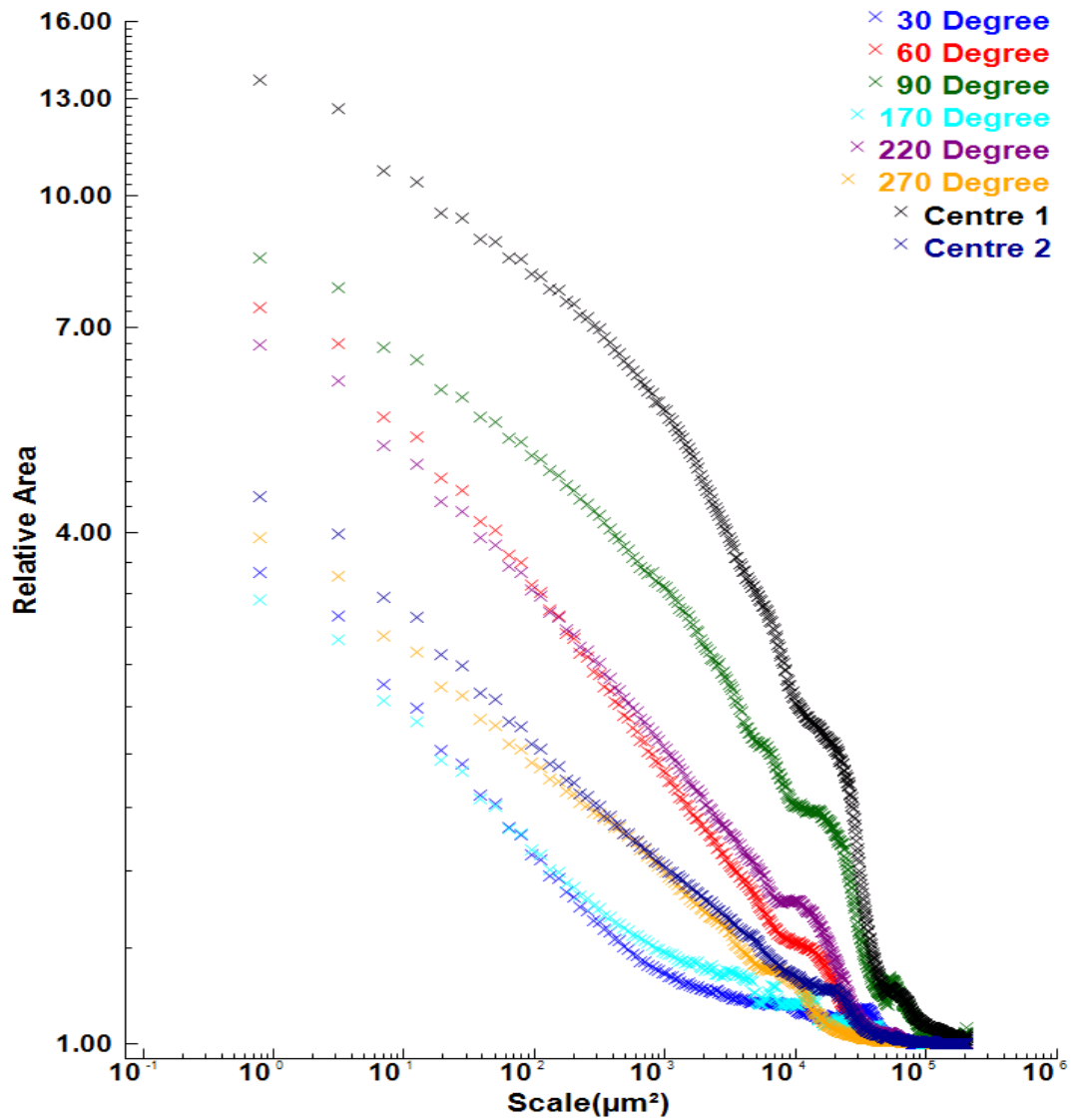


Figure 3.12: 30 over old ball, Area-scale, unfiltered

Figure 3.13 shows the Area-scale plots after using the spike removal tool from OLYMPUS. The 30, 170, 270 and center 1 measurements have the highest relative area higher than 2 whereas the rest of the measurements have unrealistic relative areas which shows that this filtering technique did not remove the majority of spikes for most of the measurements.

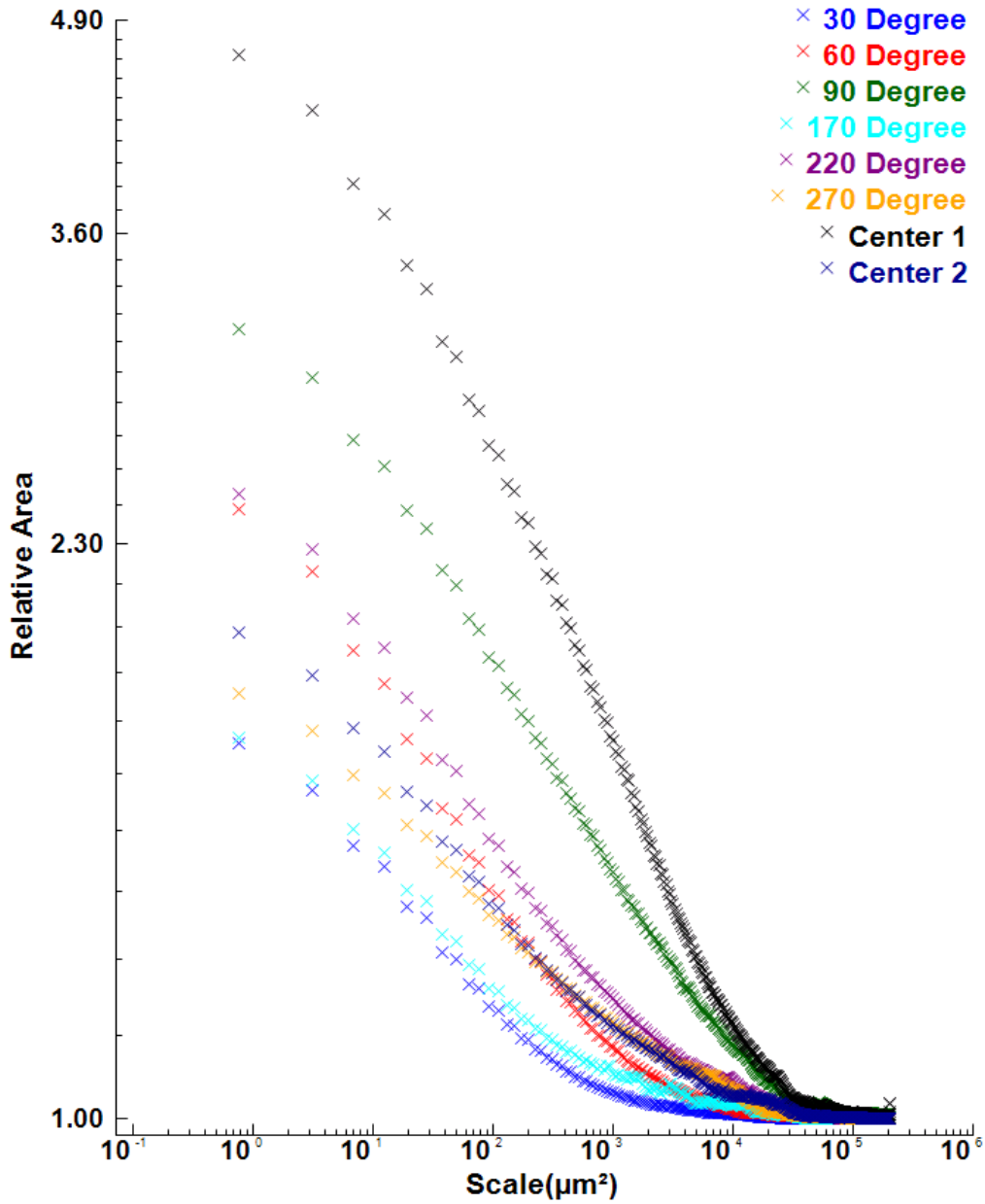


Figure 3.13: 30 over old ball, Area-scale with spike removal

Figure 3.14 shows the Area-scale plots for the same ball but after employing the Gauss filter. The highest relative is between 1.55 and 2.30 which is a big improvement from the previous plot, although relative areas higher than 2 show that there are still some

unmeasured points or spikes. The 30 over old ball was the hardest to measure because of highly surface at some locations and hence the results had a lot of spikes.

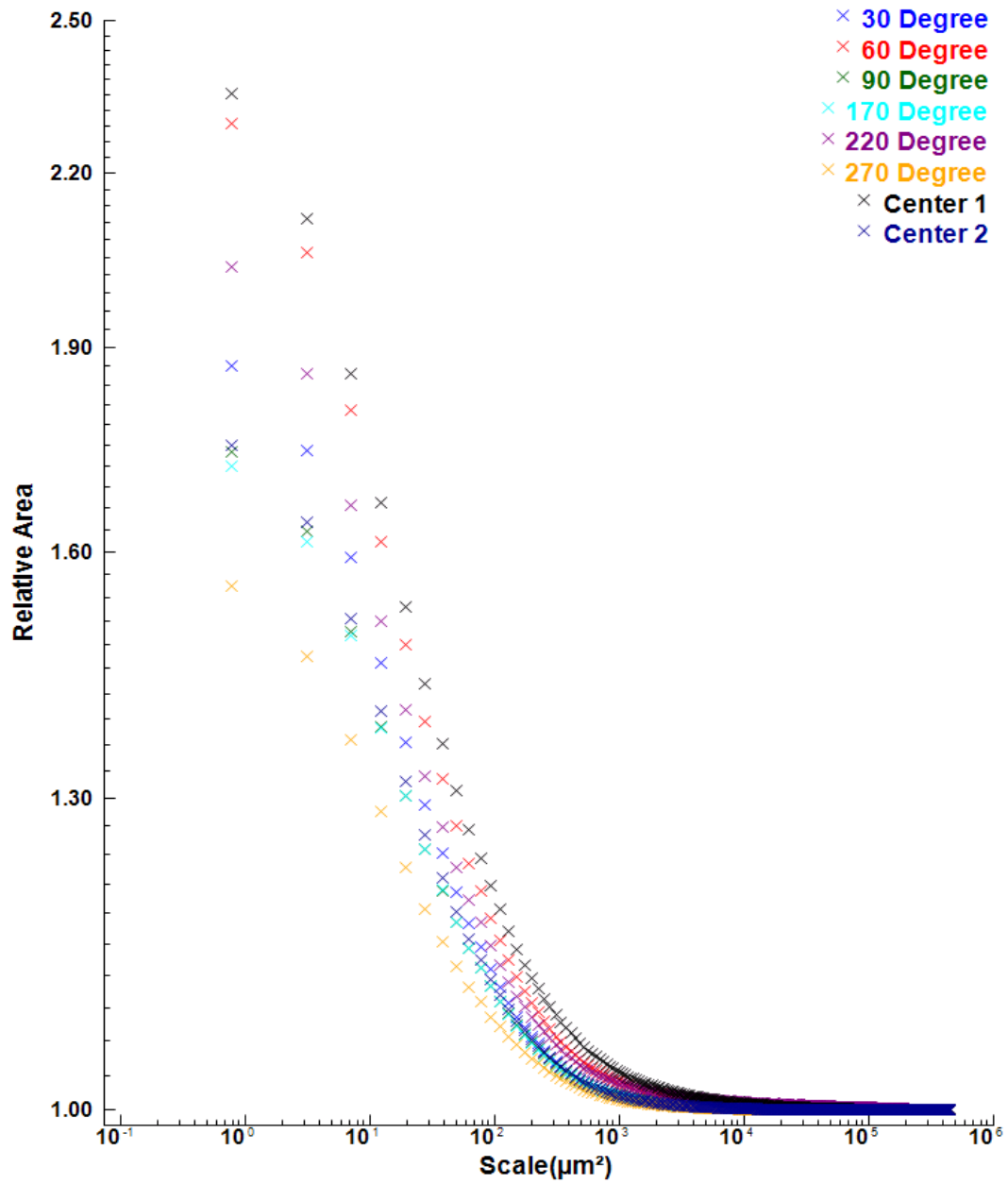


Figure 3.14: 30 over old ball, Area-scale with Gauss filter

3.4.3 50 over old ball

The following three figures show the Area-scale plots for the 50 over old ball.

Figure 3.15 shows the unfiltered Area-scale plots for the 50 over old ball. All the regions have a high relative area which shows the presence of spikes. An interesting point to point to note here is that the difference in the highest relative areas is not too much which shows that although a lot of points were lost during the measurements but the surface

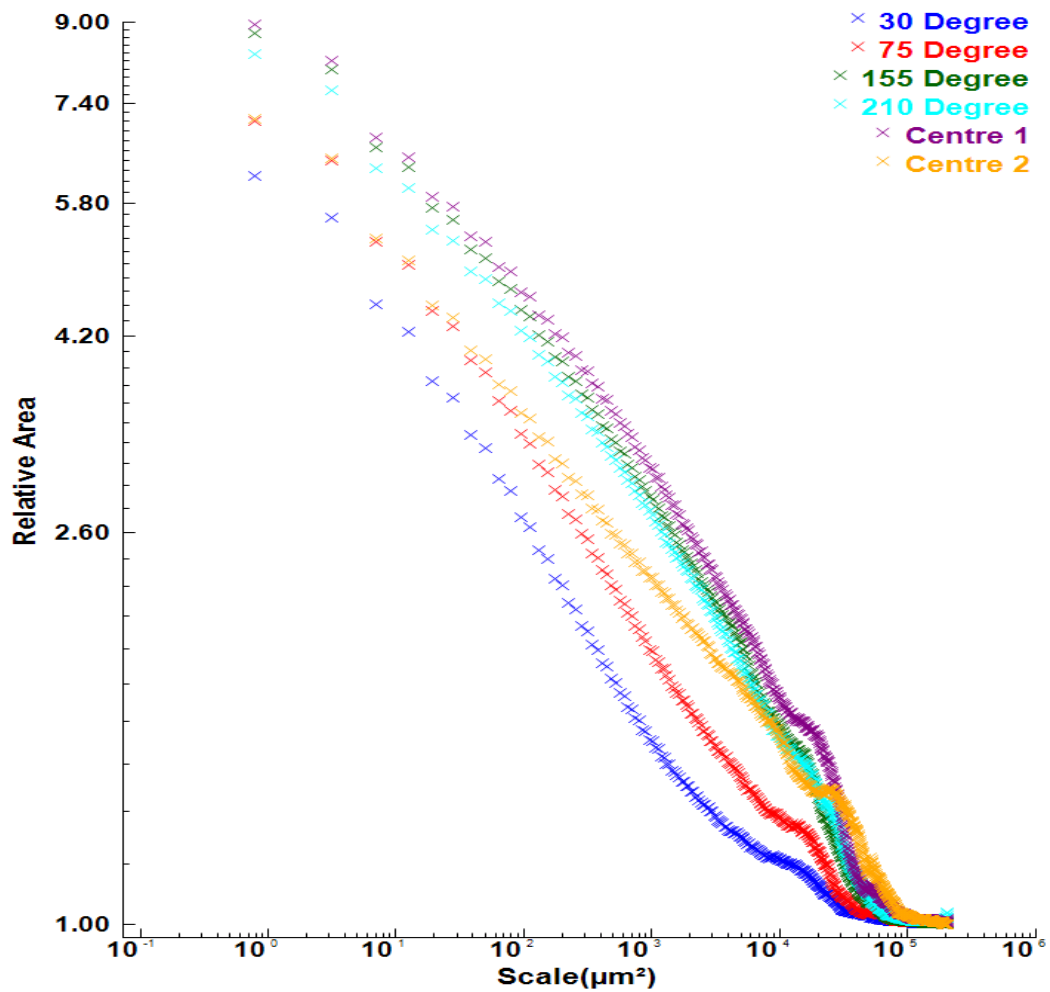


Figure 3.15: 50 over old ball, Area-scale, unfiltered

texture is the same around the circumference of the ball. This fact is evident by simply looking at the ball too.

Figure 3.16 shows the Area-scale plots for the same ball after using the spike removal tool provided in the OLYMPUS software.

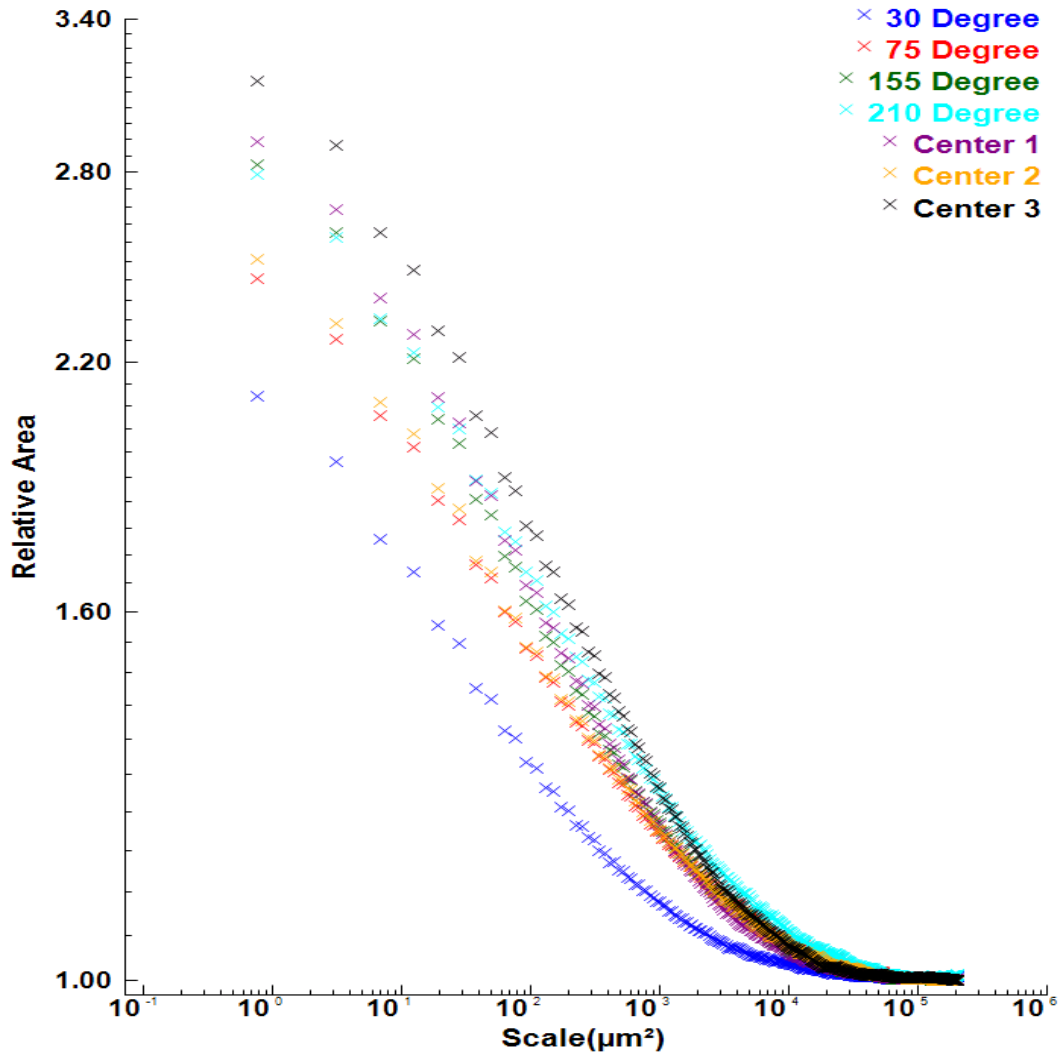


Figure 3.16: 50 over old ball, Area-scale with spike removal

The relative area values have decreased significantly but they are still above 2 which show that the spike removal tool has not removed most of the spikes.

Figure 3.17 show the Area-scale plots for the same ball after employing the 5 um Gauss filter using MOUNTAINS. The highest relative areas lie between 2.20 and 2.35 which show that the surface is rough but the texture is similar.

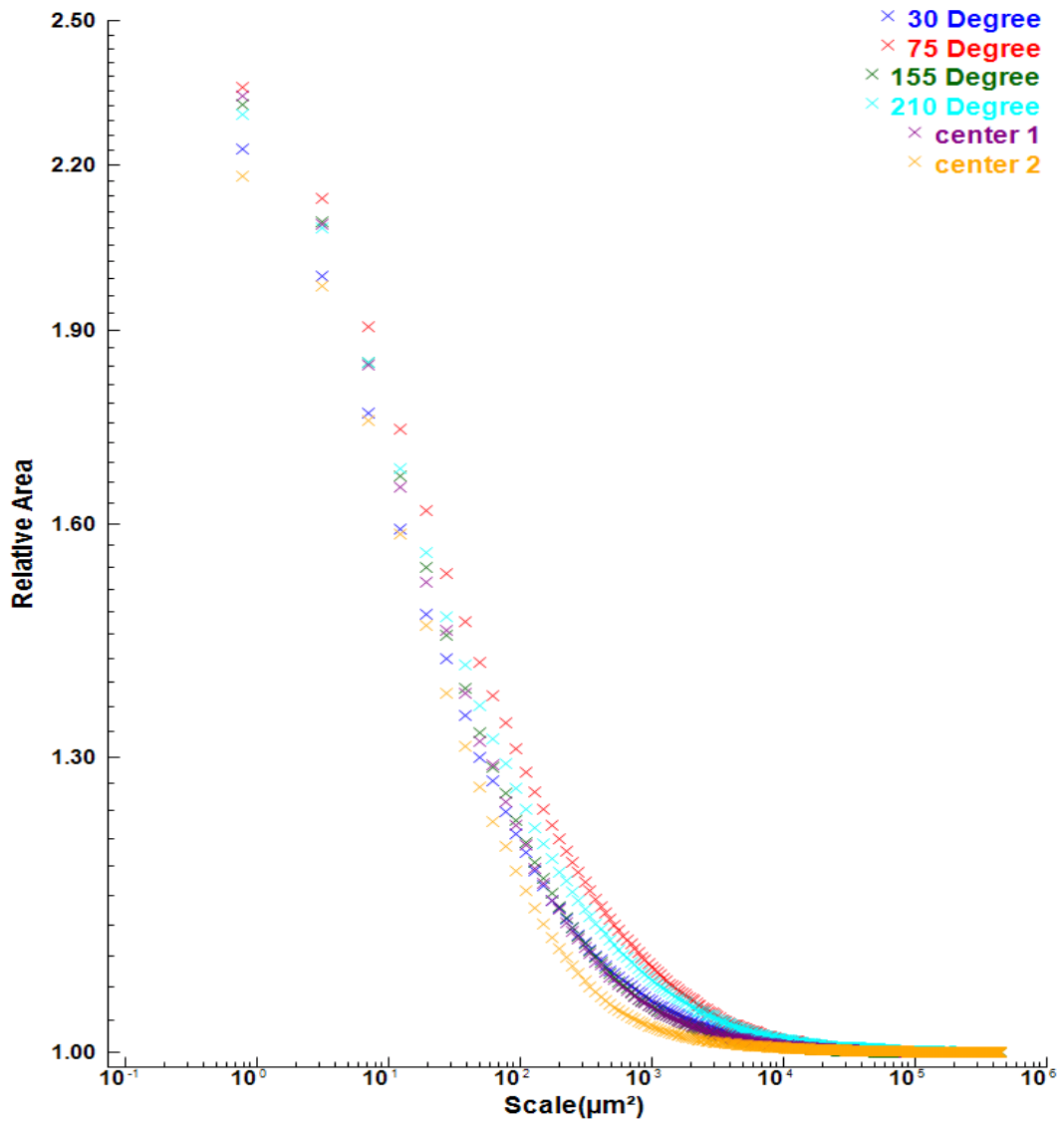


Figure 3.17: 50 over old ball, Area-scale with Gauss filter

3.5 Comparison of Area-scale fractal analysis

The mean values of Area-scale results for the unfiltered results are shown in figure 3.18. At higher scales it is not possible to discriminate between the balls. The new ball can be discriminated from the other two at a scale of $5500 \mu\text{m}^2$. The old and 50 over old ball can be discriminated at a fine scale of $500 \mu\text{m}^2$.

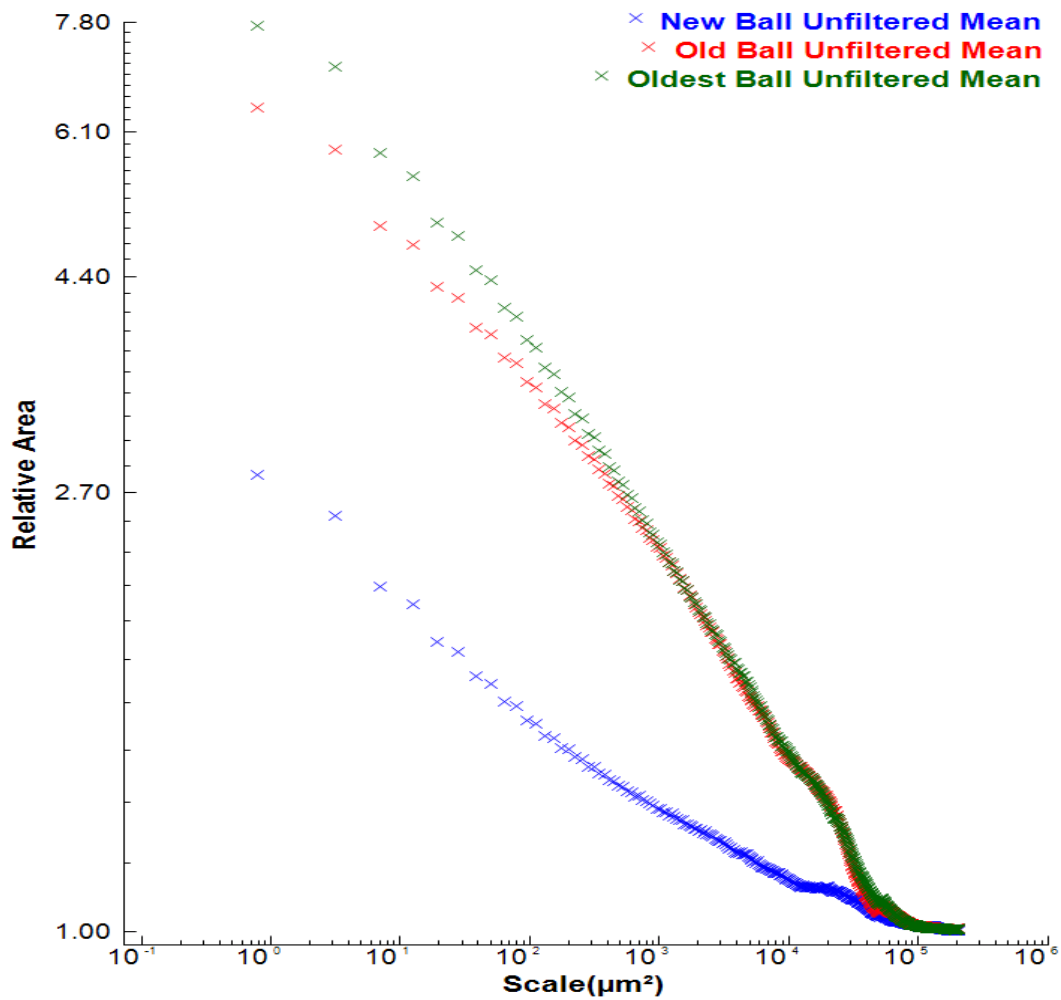


Figure 3.18: Comparison of Area-scale, mean, unfiltered

The mean values of Area-scale results after spike removal are shown in figure 3.19. The new ball can be discriminated from the other two at a scale of $5500 \mu\text{m}^2$. The old and the 50 over old ball are impossible to be discriminated at high scales. At a fine scale of $10\mu\text{m}^2$ the Area-scale curves start to deviate and hence there's some level of discrimination.

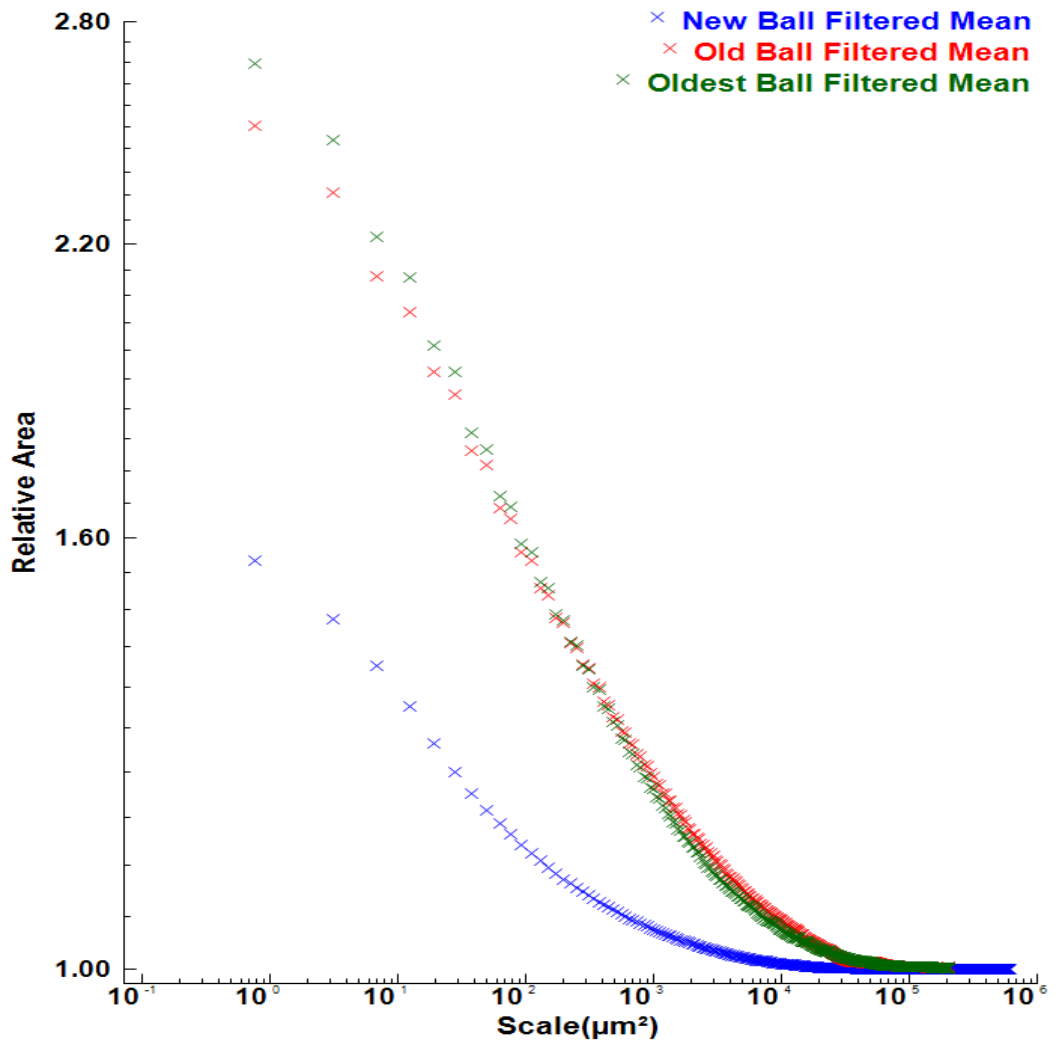


Figure 3.19: Comparison of Area-scale, mean with spike removal

The mean values of Area-scale results after using a Gauss filter are shown in figure 3.20. The old and 50 over old ball can be discriminated at a scale of $5500 \mu\text{m}^2$. The 50 over old ball can be discriminated from the new ball at the same scale. Whereas the new ball can be discriminated from the 30 over old ball at a finer scale of $800 \mu\text{m}^2$

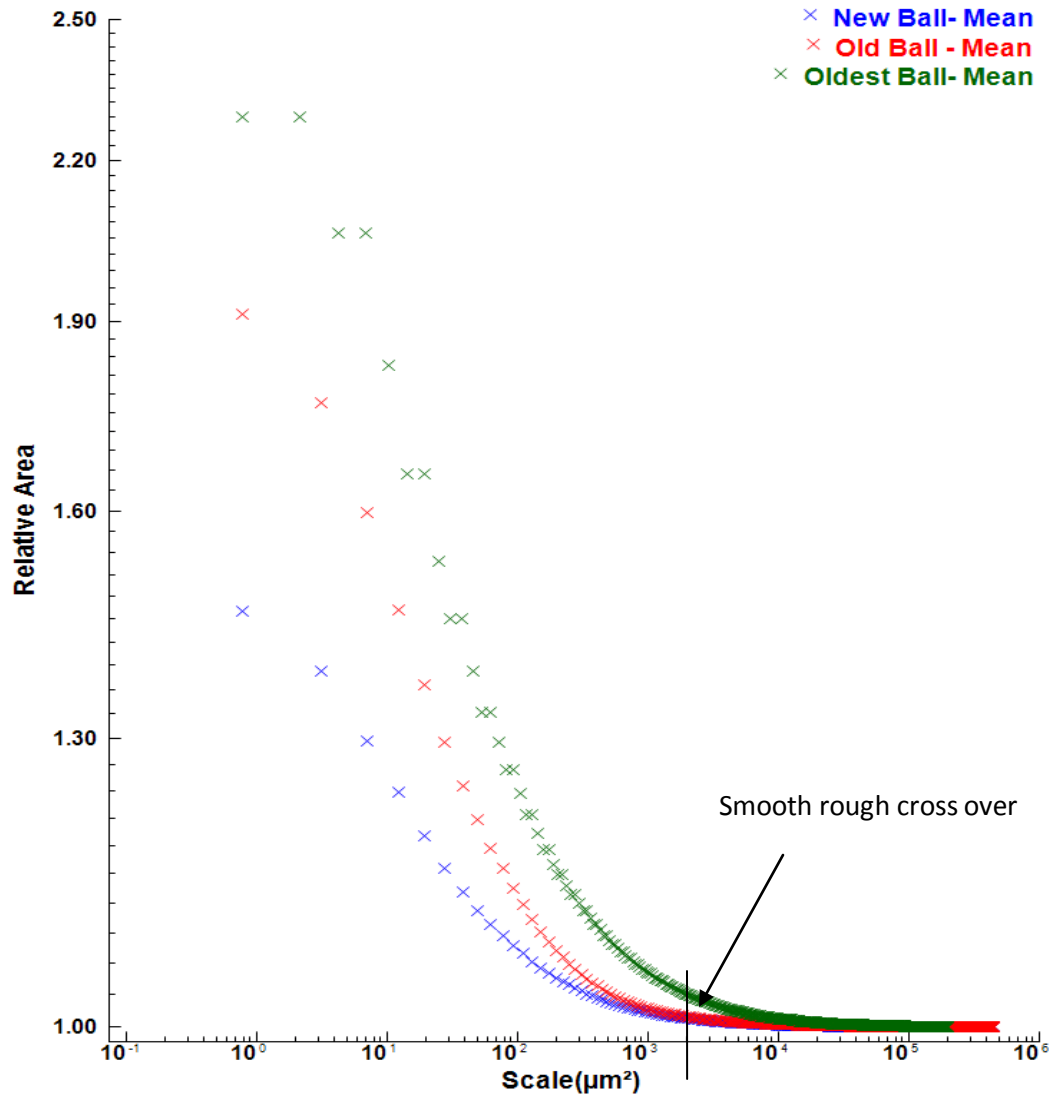


Figure 3.20: Comparison of Area-scale with Gauss filter

3.6 FTEST

F-Test results of mean values of Area-scale analysis for a 90 % confidence level are presented in the following three figures. All of these results are for the measurements which have been filtered using a Gauss filter.

Figure 3.21 shows the results for new and 30 over old balls. At higher scales the mean square ratio is low and hence it is not possible to discriminate between the two balls.

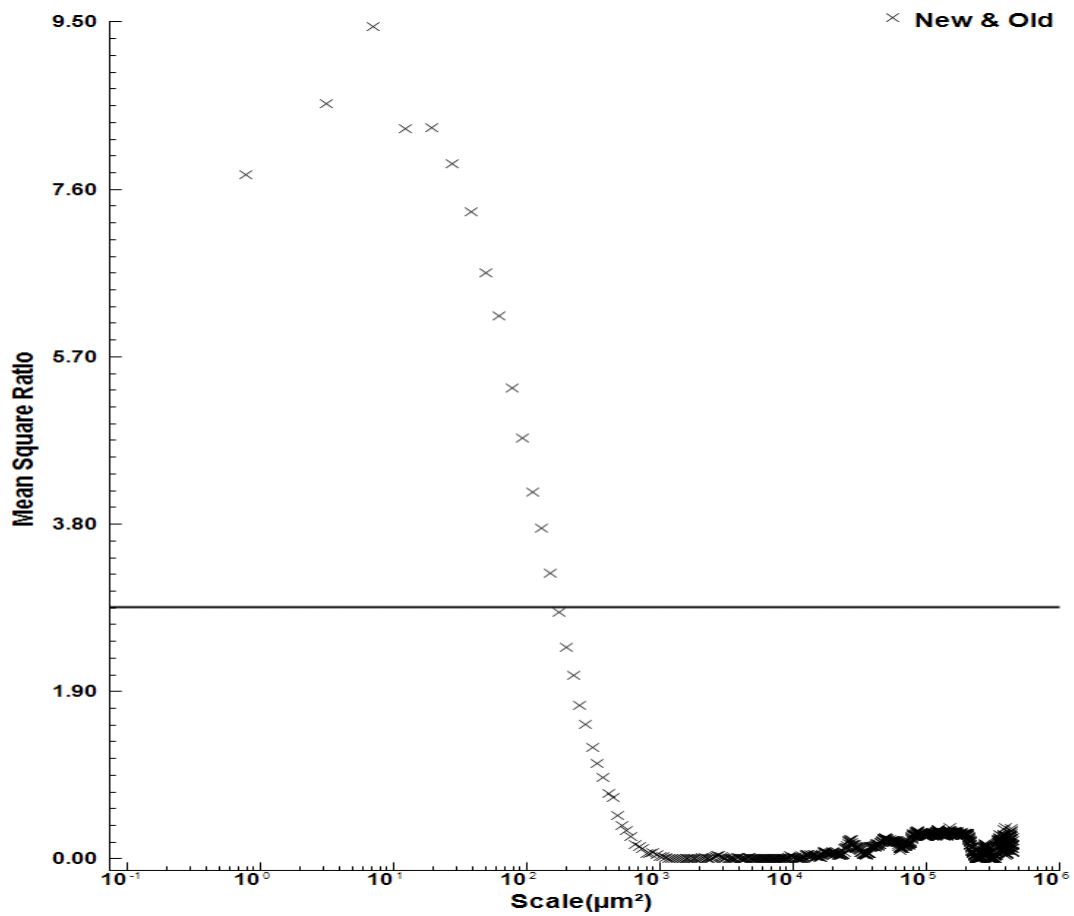


Figure 3.21: FTEST, mean, Area-scale, new vs. old with 90% confidence

At scales lower than $150 \mu\text{m}^2$ the mean square ratio becomes higher than the minimum MRS value (2.85) for a 90 % confidence level and hence we can discriminate.

Figure 3.22 shows the results for new and 50 over old ball. The mean square ratio at all scales is high and the two balls are highly different hence making it easy to discriminate.

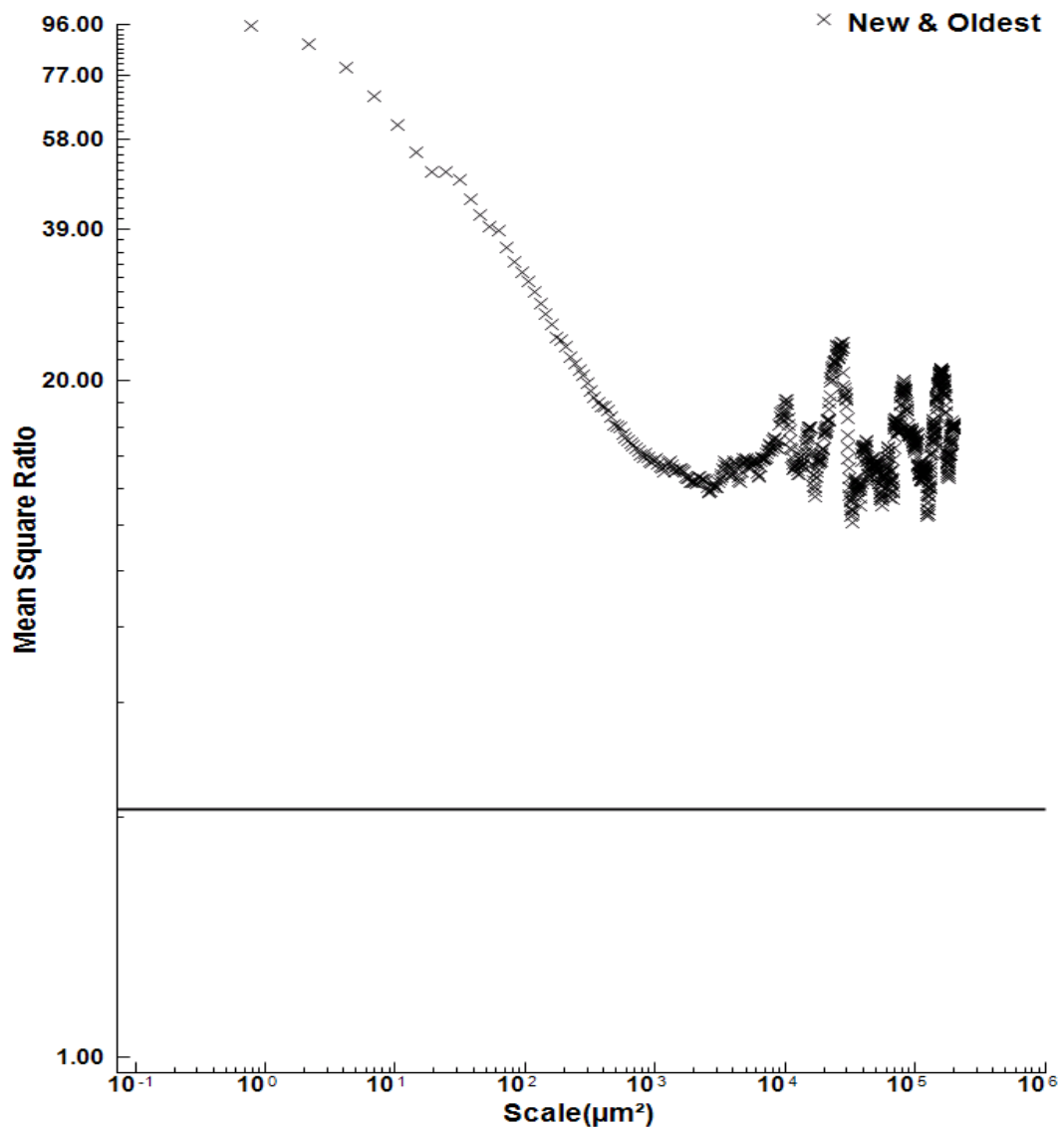


Figure 3.22: FTEST, mean, Area-scale, new vs. oldest with 90% confidence

Figure 3.23 shows the F-Test results for the new and 50 over old ball. At higher scales it the mean square ratio has a low value and hence it is not possible to discriminate. At scales finer than $82500 \mu\text{m}^2$ the mean square ratio becomes higher than the minimum value (2.85) for a 90 % confidence level and hence the balls can be discriminated.

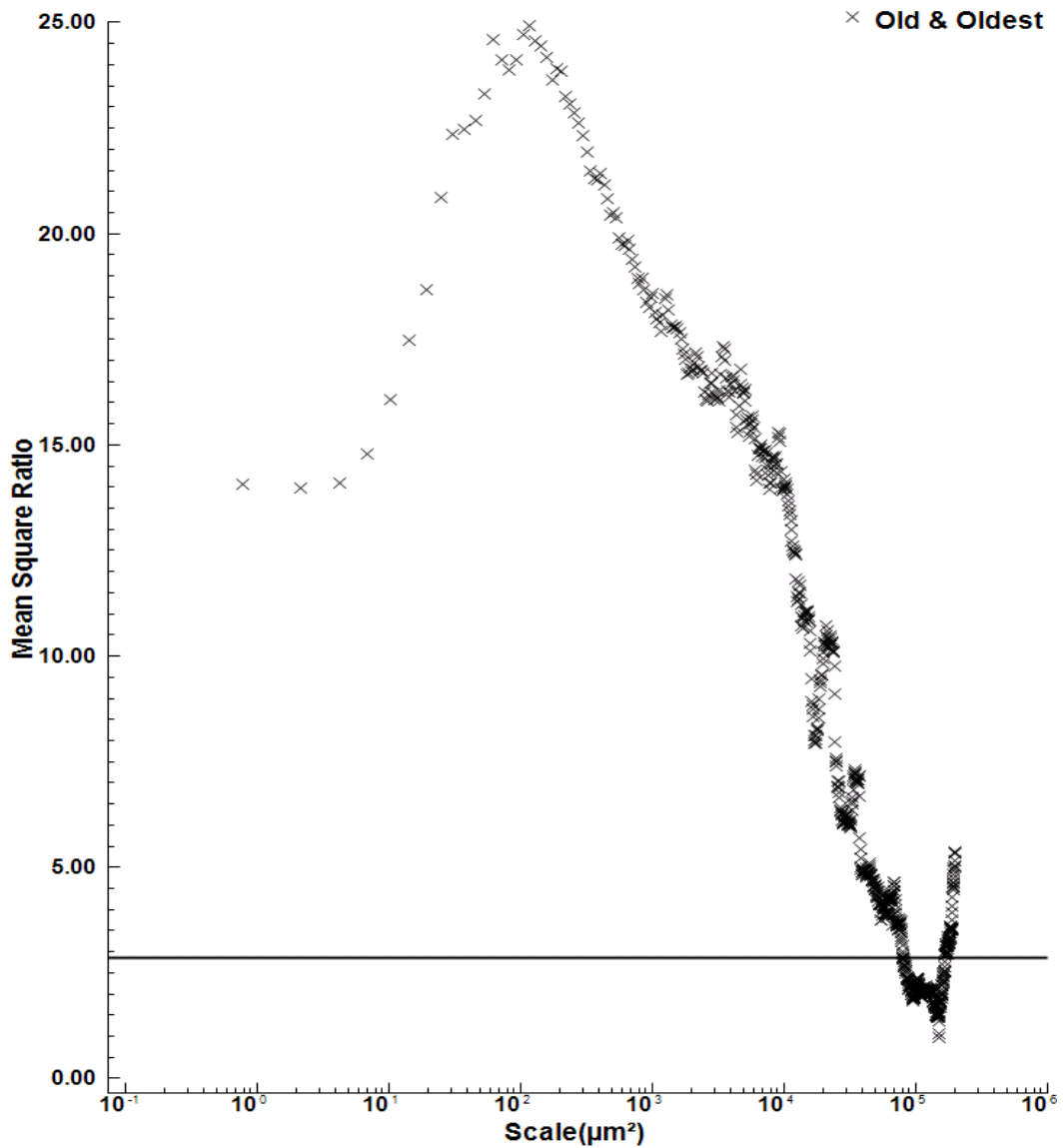


Figure 3.23: FTEST, mean, Area-scale, old vs. oldest with 90% confidence

3.7 Wind tunnel tests

Wind tunnel results for the three balls are shown below. Speed is plotted against drag coefficient in figure 3.24. The C_D for the new ball increases initially up till 75 mph but after that there is a steady decrease in it. For the 30 over old ball C_D increases with speed and for the 50 over old ball it keeps increasing and decreasing with increasing velocity. It is evident from the C_D values that there isn't a significant increase for the 50 over old ball.

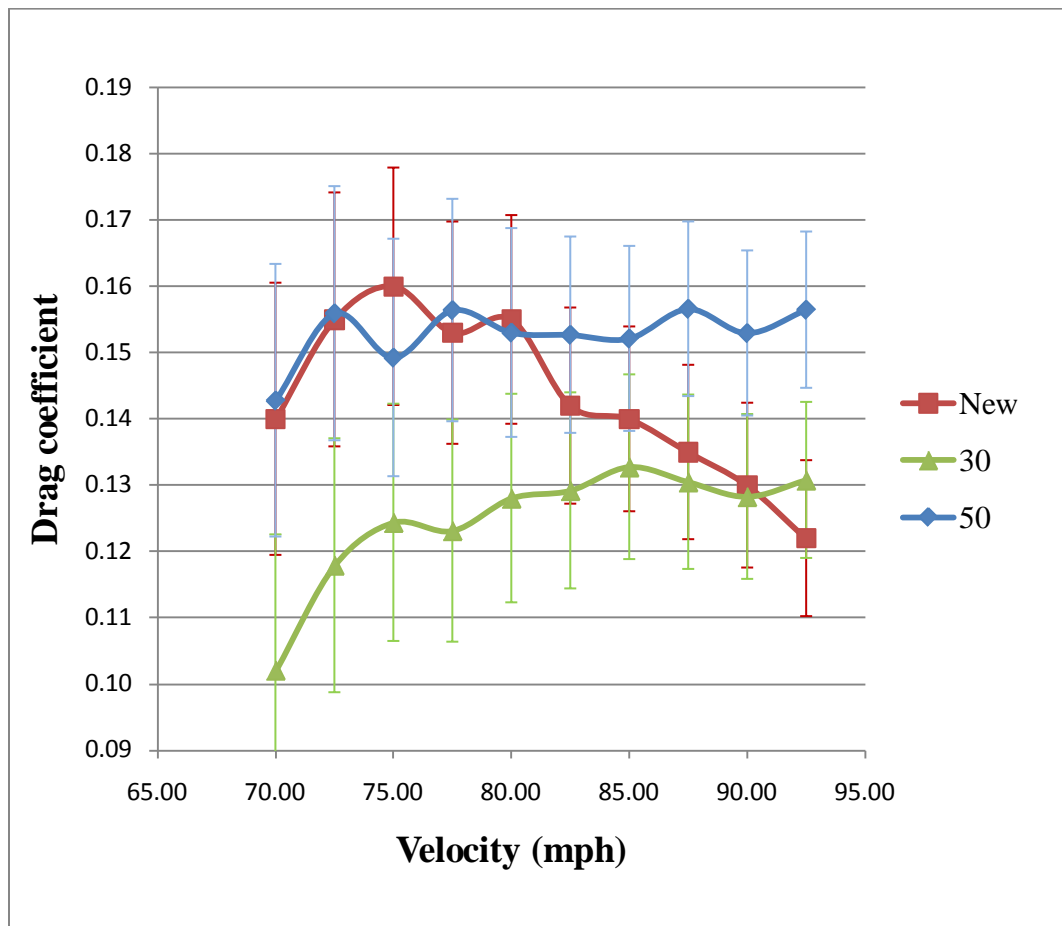


Figure 3.24: Velocity vs. drag for the cricket balls

The data acquisition system for the wind tunnel returns values with two significant digits. An uncertainty test is done to compute the minimum and maximum values of C_D for the three cricket balls using the following equations and the results are shown in figure 3.24 using the error bars.

$$C_{D_{max}} = \frac{2(F_D + 0.05)}{\rho A(V - 0.05)^2}$$

$$C_{D_{min}} = \frac{2(F_D - 0.05)}{\rho A(V + 0.05)^2}$$

Where;

C_D = Coefficient of drag

F_D = Drag

V = Velocity

ρ = Density of air

A = Area of the cricket ball

3.8 Relationship between drag and roughness

In order to correlate drag and roughness of cricket balls the coefficient of correlation is calculated at each scale. Figure 3.25 shows the calculation of R^2 (coefficient of correlation) for one drag value at a certain velocity with a changing relative area. This exercise is repeated for various scales and drag values to get figure 3.26. The values this R^2 range between 0 and 1. It is a measure of how well the drag and relative are correlated. A higher value indicates a better correlation.

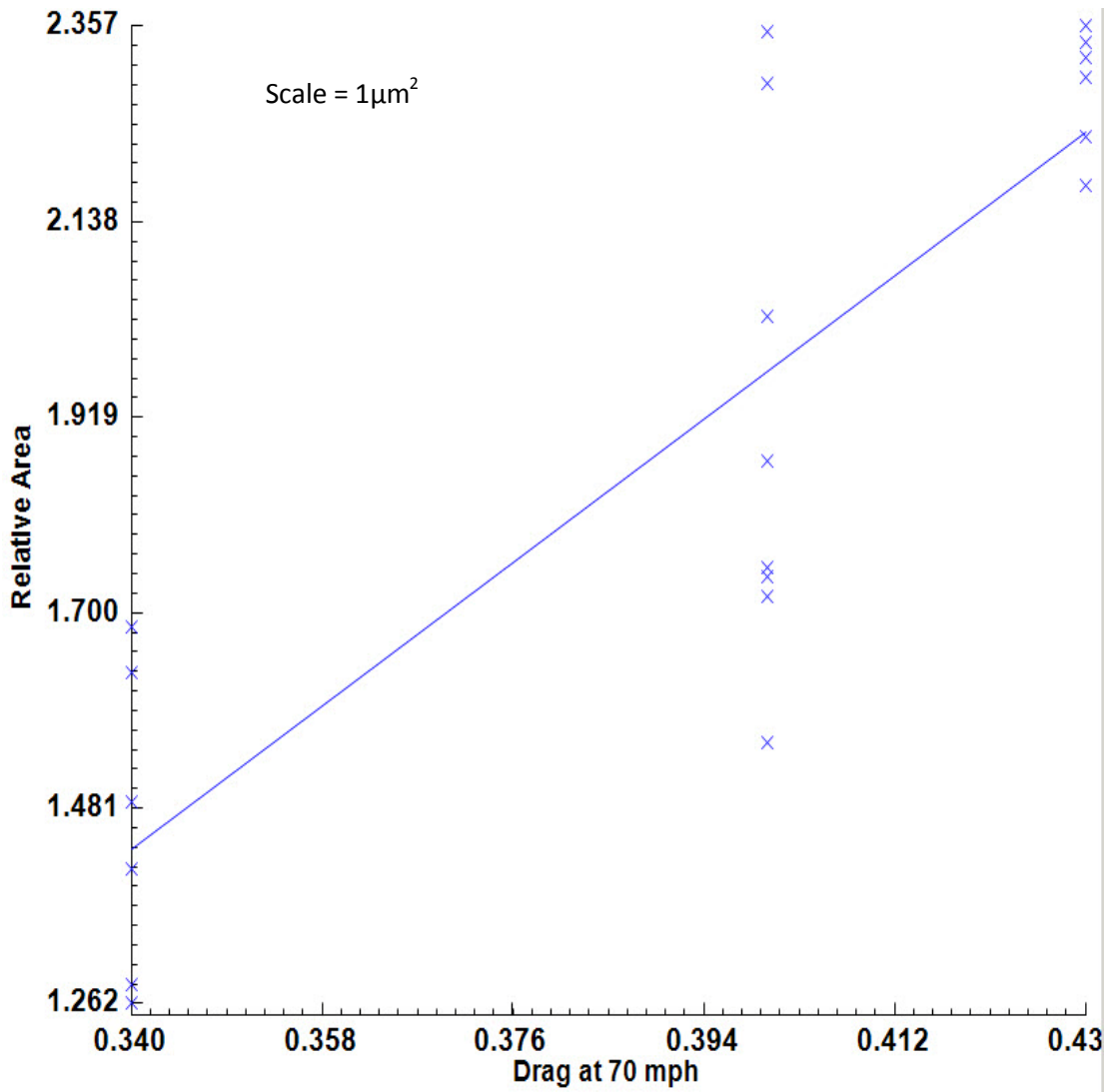


Figure 3.25: Regression plot showing the calculation of R^2 for drag vs. relative area

Figure 3.26 shows the correlation between drag and relative area calculated at each scale. The scale at which the relative area becomes significantly greater than 1 is known the smooth rough cross over (SRC). Before the SRC any high values of R^2 are insignificant. After the SRC we a high correlation between the drag and relative area at velocities of 70, mph, 72.5 mph, 90 mph and 92.5 mph between the scales of $10\mu\text{m}^2$ and

$500 \mu\text{m}^2$. The highest R^2 is at a scale of $200 \mu\text{m}^2$ for the drag at 92.5 mph and at $20 \mu\text{m}^2$ for the drag at 70 mph.

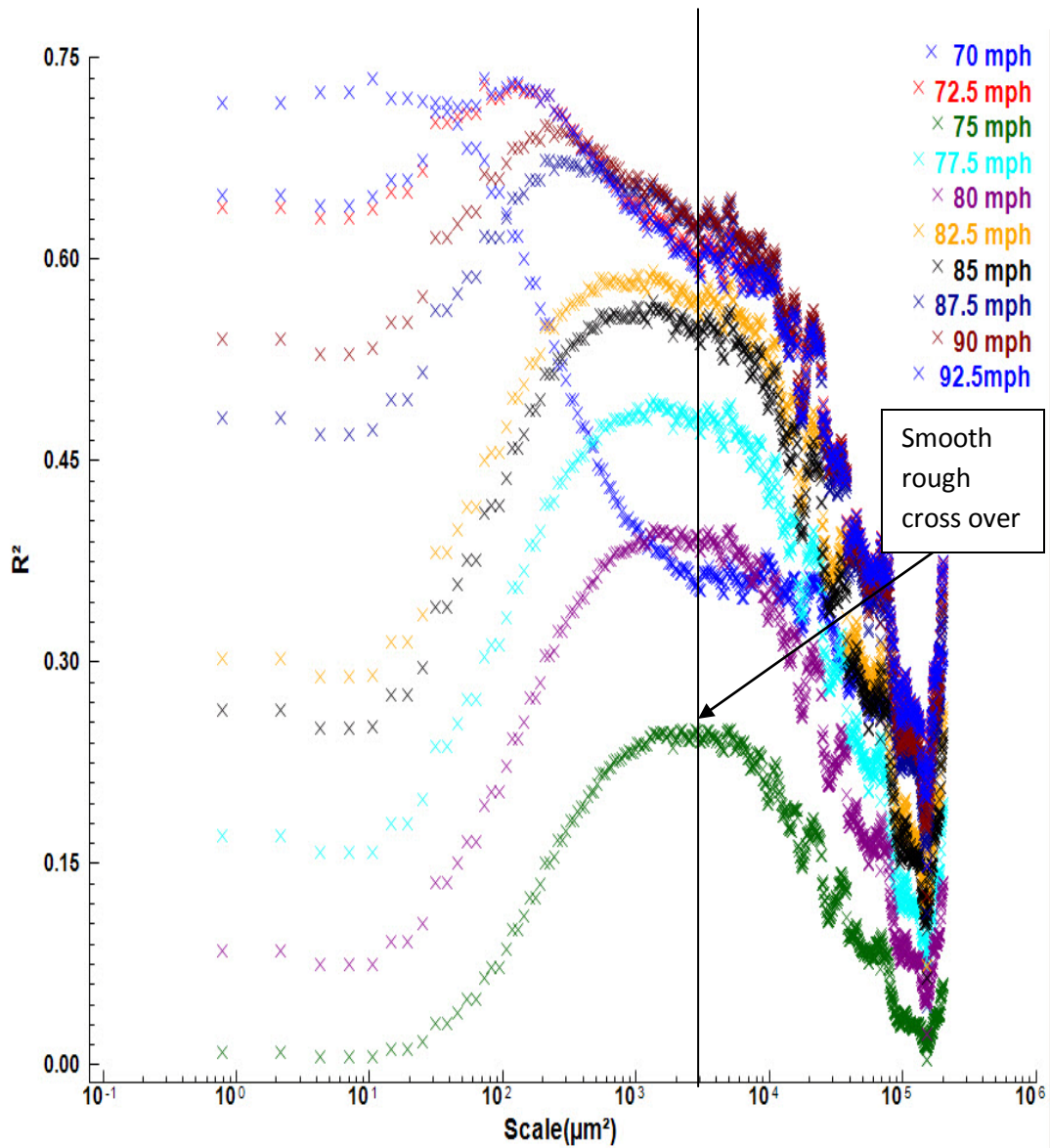


Figure 3.26: Drag at different velocities vs. relative area

Figure 3.27 shows the relationship between C_D and relative area. Higher values of R^2 are observed for C_D at 70mph and 92.5 mph at scales of $20 \mu\text{m}^2$ and $200 \mu\text{m}^2$ respectively. Once again the high values of R^2 before the SRC are not significant because the relative area is equal to 1 in that region.

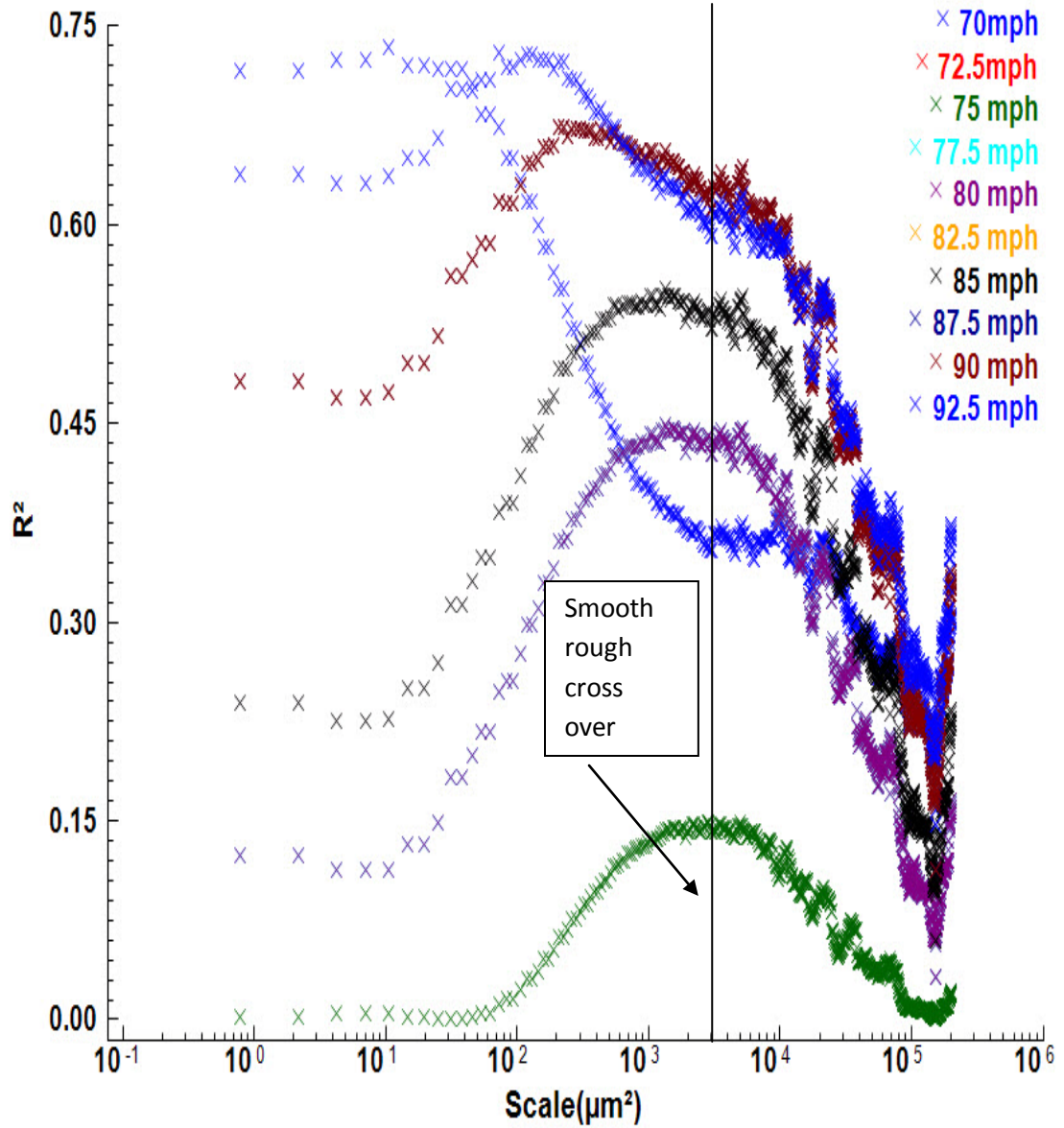


Figure 3.27: C_D at different velocities vs. relative area

Chapter 4

Discussion

In this section theories about the relationship of surface roughness and aerodynamic behavior are discussed and an attempt is made to relate the surface texture characterization presented in the previous chapters to the aerodynamic behavior of cricket balls observed from wind tunnel tests. The Area-scale plots discussed in this section are the ones obtained after using the Gauss filter.

Surface roughness measurements for new and 30 over old balls were presented in the previous chapters and an attempt was made to discriminate between the three balls using relative area and the FTEST. Figure 3.1 shows the micrographs of the new ball at different locations. The surface looks similar with dents evident at various locations. The surface of the balls is tried to be made as spherical as possible and it looks like tool marks used for that purpose. The relative area for the new ball shown in Figure 3.11 is much less than that for the old and 50 over old ball and the values of relative areas at various locations around the circumference of the ball are not too different. This shows that the surface texture is similar which is easy to correlate to the playing performance of a new ball. A new ball's surface is smooth and the seam is used primarily to make it swing.

Figure 3.2 shows the micrographs for the 30 over old ball. It's evident that the ball loses the top shiny surface as the time goes on. The images show the propagation of a crack and the appearance of 50 over old ball like structure. The relative areas for the 30 over old ball have a higher value as compared to the 30 over old ball. Also the difference

in relative area for different regions is large. It looks like the higher relative area measurement was made at a spot which is more like the 50 over old ball. The highest relative area for the 30 over old ball shown in figure 3.14 is above 2 which confirms the comment made earlier that the region is much rougher.

According to the theory on aerodynamic performance of cricket balls (Mehta et al, 1983), as the ball becomes rough, the bowler shines one side of the ball and lets the other side get rough. As the ball travels through air the boundary layer on the smooth side is laminar and on the rough side it's turbulent. The turbulent boundary layer tends to stick to the surface of the ball a bit longer than the laminar one. The separation point of the stream lines behind the ball on the smooth side is a bit earlier than the rough side which produces a side force and hence the ball exhibits reverse swing. This type of swing is observed only once the ball has become rough on one side. The relationship of this behavior with our measurements is evident. The combination of rough and smooth regions for a 30 over old ball gives rise to a turbulent boundary layer on the rough side.

The 50 over old ball seems to have a similar texture all around the circumference. The conventional roughness parameters have a high value as compared to the new and old one. The relative area is also high which confirms the hypothesis that it is rougher than the new and old one. It is easy to discriminate from the other two on the basis of these results along with the FTEST. The relatively low lateral movement exhibited by 30 over old balls during a game is attributed to the fact that the texture doesn't have rough and smooth regions and hence the difference in texture of smooth and rough sides is not

pronounced anymore to give rise to laminar and turbulent boundary layers on respective sides.

The wind tunnel results shown in figure 3.24 show a slight increase in C_D for the 50 over old ball. From literature survey the C_D for a smooth sphere is 0.1 and for a rough one its 0.4. The increase in C_D with a corresponding increase in velocity is not that significant and also C_D values for the new ball start decreasing with an increase in velocity. In order to understand the reason, the number of significant digits displayed by the data acquisition system was taken under consideration. Maximum and minimum values of C_D were calculated based on the error as shown in figure 3.24 with the error bars.

The relationship between drag and relative area is shown in figure 3.26. The correlation can be established for velocities of 70 mph, 72.5 mph, 90 mph and 92.5 mph because of the high value of R^2 which serves as the correlation coefficient. Thus based on the current experiments a correlation can be drawn between drag and relative area for certain velocities. In figure 3.27 the correlation between C_D and relative area is shown. Here we get a value of 0.74 for R^2 at a scale of $20 \mu\text{m}^2$ which establish the highest correlation. At 92.5 mph, the value of R^2 is 0.73 but at a scale of $500 \mu\text{m}^2$.

Chapter 5

Conclusions and recommendations

A conventional surface roughness parameter S_a is used to discriminate between the balls and based on the TTEST it is established the balls can be discriminated.

Area-scale fractal analysis proves to be a good method to establish a discrimination criterion for the cricket ball surface texture.

Scale based FTESTS provide enough information for discrimination between the balls.

Wind tunnel tests performed on the three balls show a difference in C_D for the three balls. A detailed study of the aerodynamic behavior of cricket balls of various ages is required to establish a relationship between the roughness and the amount of swing produced. C_D provides some information about this relationship but a look at the boundary layer for new and old balls seems to be a better way to understand the phenomenon. Future studies to continue this work will include a detailed study of the boundary layer using flow visualization techniques like particle image velocimetry.

The correlation studies between relative area and the drag provide information for some velocities. It appears that at larger scales before the smooth rough cross over there is some correlation but it's not significant because the relative area is below 1 in that region. Hence it is concluded that the wind tunnel results need to be improved in order to establish a better correlation.

An interesting way of using the present study will be to find the difference in surface roughness of red and white cricket balls. It is known from experience that a white ball wears quickly as compared to a red one. A quantified measure of roughness of both types of balls will be valuable.

A comparison between cricket balls manufactured by different companies will be an interesting study too. Some players like Australian manufactured balls but the subcontinent players tend to prefer the local cricket balls. The reason being Australian balls (e.g. Kookaburra) are manufactured for bouncy Australian pitches and they tend to not perform according to the liking of subcontinent bowlers due to the variable bounce dryer pitches in India, Pakistan and Sri Lanka.

References

1. Barton, N. (1982). "On the swing of a cricket ball in flight," *Proceedings of the Royal Society of London. Series A, Mathematical and Physical Sciences*, 109-131.
2. C.A. Brown, Butland, R.M., Johnsen, W.A., "Scale-Sensitive Fractal Analysis of Turned Surfaces," *Annals of the CIRP*, Vol. 45, No.1, 515-8, (1996).
3. C.A. Brown, "Guide to Length Scale and Area-scale Analysis in surface Metrology," (2005).
4. C.A. Brown, P.D. Charles, W.A. Johnsen, S. Chesters, "Fractal Analysis of Topographic Data by the Patchwork Method," *Wear*, 161 (1993) 61-67
5. Cooke, J. C. (1955). "The boundary layer and seam bowling," *The Mathematical Gazette*, (39), 196-199.
6. Haake, S. J., Goodwill, S. R. and Carre, M. J. (2007). "A new measure of roughness for defining the aerodynamic performance of sports balls," *Proceedings of the Institution of Mechanical Engineers, Part C: Journal of Mechanical Engineering Science*, 221(7), 789-806.
7. James D.M., Carre M.J. and Haake S.J. (2004) "The playing performance of county cricket pitches," *Sports Engineering*, 7, 1, 1-14.
8. Kensington, A. (1982). "On the swing of a cricket ball in flight," *Proceedings of the Royal Society of London. Series A, Mathematical and Physical Sciences*, 379(1776), 109-131.
9. Lipscon C. and Sheth J. N. "Statistical design and analysis of engineering experiments" *McGraw-Hill*, 1973.

10. Lyttleton, R. A. (1957). "The swing of a cricket ball," *Discovery*, (18), 186-194.
11. Mehta, R.D. and Wood, D.H. (1980). "Aerodynamics of the cricket ball," *New Scientist*, 87(1213), 442-447.
12. Mehta, R.D., Bentley, K., Proudlove, M., & Varty, P. (1983). "Factors affecting cricket ball swing," *Nature*, 303, 787-788
13. Mehta R.D., Brown W. (1993). "The seamy side of swing bowling *New Scientist*, 187, No. 1213.
14. Mehta, R. D. (2005). "An overview of cricket ball swing," *Sports Engineering*, 8(4), 181-192.
15. Newton, I. (1672). "New theory of light and colours," *Phil. Trans. R. Soc.*, 1, 678-688.
16. Rayleigh, L. (1877). "On the irregular flight of a tennis ball," *Messenger of Mathematics*, (7), 14-16.
17. Sayers, A., & Hill, A. (1999). "Aerodynamics of a cricket ball," *Journal of Wind Engineering & Industrial Aerodynamics*, 79(1-2), 169-182.